Stem Cell Reports
Resource
OPEN ACCESS

Transcriptome-wide Analysis Reveals Hallmarks of Human Intestine Development and Maturation In Vitro and In Vivo

Stacy R. Finkbeiner,[1,2] David R. Hill,[1] Christopher H. Altheim,[1] Priya H. Dedhia,[2,5] Matthew J. Taylor,[3] Yu-Hwai Tsai,[1] Alana M. Chin,[4] Maxime M. Mahe,[6] Carey L. Watson,[6,7] Jennifer J. Freeman,[2,5] Roy Nattiv,[8] Matthew Thomson,[11] Ophir D. Klein,[8,9,10] Noah F. Shroyer,[12] Michael A. Helmrath,[6,7] Daniel H. Teitelbaum,[2,5] Peter J. Dempsey,[13] and Jason R. Spence[1,2,4,*]

[1]Division of Gastroenterology, Department of Internal Medicine
[2]Center for Organogenesis
[3]Department of Molecular and Integrative Physiology
[4]Department of Cell and Developmental Biology
[5]Department of Surgery
University of Michigan Medical School, Ann Arbor, MI 48109, USA
[6]Department of Pediatric General and Thoracic Surgery, Cincinnati Children's Hospital Medical Center, Cincinnati, OH 45229, USA
[7]Department of General Surgery, University of Cincinnati, Cincinnati, OH 45229, USA
[8]Institute for Human Genetics and Department of Pediatrics
[9]Program in Craniofacial and Mesenchymal Biology
[10]Center for Craniofacial Anomalies
[11]Center for Systems and Synthetic Biology
University of California, San Francisco, San Franciso, CA 94143, USA
[12]Department of Medicine Section of Gastroenterology and Hepatology, Baylor College of Medicine, Houston, TX 77030, USA
[13]Department of Pediatrics, University of Colorado, Denver, CO 80204, USA
*Correspondence: spencejr@umich.edu
http://dx.doi.org/10.1016/j.stemcr.2015.04.010

SUMMARY

Human intestinal organoids (HIOs) are a tissue culture model in which small intestine-like tissue is generated from pluripotent stem cells. By carrying out unsupervised hierarchical clustering of RNA-sequencing data, we demonstrate that HIOs most closely resemble human fetal intestine. We observed that genes involved in digestive tract development are enriched in both fetal intestine and HIOs compared to adult tissue, whereas genes related to digestive function and Paneth cell host defense are expressed at higher levels in adult intestine. Our study also revealed that the intestinal stem cell marker *OLFM4* is expressed at very low levels in fetal intestine and in HIOs, but is robust in adult crypts. We validated our findings using in vivo transplantation to show that HIOs become more adult-like after transplantation. Our study emphasizes important maturation events that occur in the intestine during human development and demonstrates that HIOs can be used to model fetal-to-adult maturation.

INTRODUCTION

Three-dimensional in vitro models of the human intestine, such as human intestinal organoids (HIOs), offer immense promise for gastrointestinal (GI) research. HIOs offer the unique ability to understand physiologic interactions of the intestine in an in vitro setting and have potential for future applications in tissue engineering and regenerative medicine. Reports include the use of HIOs for studying viral infections (Finkbeiner et al., 2012), bacterial infections (Leslie et al., 2015), inflammatory bowel disease (Xue et al., 2013), and development of enteroendocrine and β cells (Chen et al., 2014; Du et al., 2012). HIOs are generated using directed differentiation of human pluripotent stem cells (hPSCs) in a stepwise differentiation process that mimics embryonic development (Finkbeiner and Spence, 2013; McCracken et al., 2011; Spence et al., 2011; Wells and Spence, 2014).

We previously showed that HIOs contain both mesenchymal and epithelial cell populations, including the four major epithelial cell types of the small intestine (enterocytes, goblet, Paneth, and enteroendocrine cells) as well as LGR5+ epithelial cells. Moreover, we demonstrated that some cell types were functional, absorbing peptides (enterocytes) and secreting mucin (goblet cells). These findings suggested that HIOs represent mature, functional intestinal tissue (Spence et al., 2011). This conclusion was in contrast to findings in other hPSC-derived lineages, such as pancreatic β-like cells and in lung organoids, which were shown to be more similar to fetal rather than adult tissue (Dye et al., 2015; Hrvatin et al., 2014).

Interestingly, follow-up studies by other groups and ours using HIOs have suggested that HIOs are less mature than adult tissue (Fordham et al., 2013), and HIOs transplanted into the mouse kidney capsule exhibit enhanced cellular function and morphology (Watson et al., 2014). However, the maturity of HIO tissues in vitro remained uncertain, as it was unclear if HIOs represented tissue that was fetal in nature or, alternatively, if expression levels of some genes simply remained low in vitro. Therefore, in this study we

sought to do the following: (1) investigate the developmental state of maturity of in-vitro-derived HIOs, (2) determine if HIOs are more similar to human fetal or adult intestinal tissue, and (3) identify cellular and molecular hallmarks of human intestinal maturation. Using RNA-sequencing (RNA-seq) and transcriptome-wide comparisons of HIOs, human fetal, and human adult intestinal tissue, our data show that while HIOs possess markers for functional cell types as originally reported, they are globally more similar to fetal human intestinal tissue than to adult intestine. We also show that the enhanced cellular differentiation and enhanced cellular function after in vivo engraftment of HIOs under the mouse kidney capsule correspond to mature adult-like intestinal tissue. Hallmarks of this maturation process include strong induction of antimicrobial peptide genes produced by Paneth cells and enhanced expression of genes required for digestion. We also found that expression of the Notch-dependent intestinal stem cell (ISC) marker *OLFM4* (van der Flier et al., 2009b; VanDussen et al., 2012) is very weakly expressed in HIOs and human fetal tissue, and that acquisition of high levels of OLFM4 expression in the crypt is a hallmark of intestinal maturation. This finding also was confirmed in the developing mouse intestine. Taken together, our results identify major cellular changes that take place during human fetal-to-adult intestinal maturation, demonstrate that acquisition of OLMF4 expression in the crypt is a hallmark of maturation, and highlight that HIOs are a tractable model system that represents human fetal intestinal tissue.

RESULTS

Transcriptome-wide Comparisons Reveal that HIOs More Closely Resemble Fetal Rather Than Adult Intestine

To understand the maturation status of HIOs based on global gene expression patterns, we conducted RNA-seq and compared global gene expression data obtained for undifferentiated H9 stem cells, definitive endoderm, and whole HIOs to existing RNA-seq datasets for fetal and adult human mucosa (epithelium and sub-epithelial mesenchyme) (Table S1). We employed principal component analysis (PCA) to examine variation in transcript abundance among the 23,615 genes contained in each of the RNA-seq datasets. The reduction of this highly multidimensional dataset into two dimensions, or principle components, enables the unbiased comparison and visualization of total transcriptional activity between samples. The results suggest that the HIO, human fetal, and adult transcriptomes differ substantially from embryonic stem cell (ESC) and definitive endoderm precursors (Figure 1A). Furthermore, the variation captured in the first two principal components (PC1 and PC2) demonstrates broad similarity between human GI tissues (fetal and adult) and the HIO tissue generated in vitro, suggesting a high degree of similarity in global transcriptional activity among these samples. In the PCA, HIOs clustered more closely with other fetal GI tissue, whereas adult tissues tended to cluster separately. This clustering was more apparent when PCA was conducted with HIO, fetal intestine, and adult intestine only (Figure S1). Since the variation in the larger dataset (Figure 1A) is largely driven by differences between more undifferentiated cells (ESCs and endoderm) and differentiated GI tissue, we conducted additional analyses to examine similarities between different tissues.

We conducted unsupervised hierarchical clustering of the global gene expression data, based on the Canberra distance (Figure 1B) and Spearman rank correlation (Figure 1C), to assess the relationship of HIOs to the other tissues. In both analyses, stem cells and definitive endoderm formed a distinct out-group relative to the GI tissues, consistent with PCA. Interestingly, human tissues segregate according to their maturation status (fetal or adult) rather than regional identity, consistent with previously published data in mice showing that gene expression in early embryonic stomach and intestine is remarkably similar, and that regional gene expression patterns do not occur until late fetal life (Li et al., 2009). Based on Canberra distance, HIOs shared a third-tier clade with the fetal stomach and fetal small intestine, supporting the high degree of similarity between HIOs and fetal GI tissue relative to adult GI tissue. Despite clustering with fetal stomach, it is important to note that HIOs expressed the intestine-specific marker CDX2 (Figure S3A; Spence et al., 2011). In the Spearman rank correlation (Figure 1C), HIOs also broadly grouped with fetal stomach and fetal small intestine; however, in this analysis, HIOs were most closely related to fetal small intestine. Additional analyses conducted on a targeted subset of data including only HIOs and fetal and adult small intestinal samples consistently demonstrated that HIOs were most closely related to fetal intestine (Figure S1).

To further assess the differences between adult intestine and HIOs and to examine these differences relative to those that exist when comparing adult and fetal human intestines, we carried out differential gene expression analysis (adult versus HIO and adult versus fetal). We identified genes significantly upregulated in adult tissue relative to HIOs (Table S2), and we identified the proportion of these genes that also were upregulated in adult tissue relative to fetal intestine (Table S3). We found that 2,719 genes were commonly upregulated in adult intestine relative to HIOs and fetal tissue, representing 49% of upregulated genes in the adult versus fetal comparison and 46.6% of upregulated

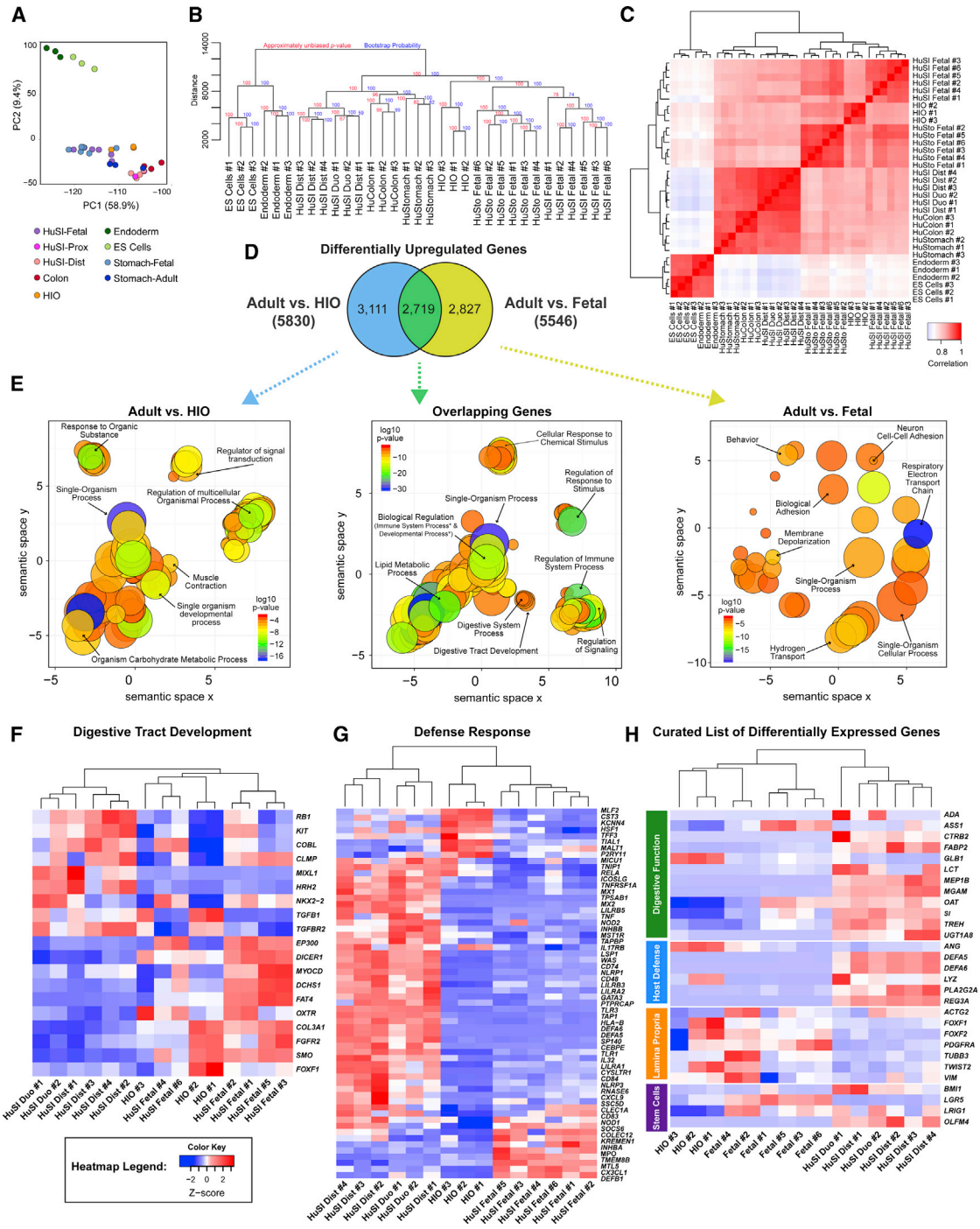

Figure 1. HIOs Resemble Fetal Intestine

(A) PCA was conducted on undifferentiated H9 ESCs (n = 3 independent experiments), definitive endoderm (n = 3 independently differentiated from H9s), HIOs (n = 3 independently differentiated from H9s), adult distal small intestine (n = 4 independent biological specimens), adult duodenum (n = 2 independent biological specimens), adult colon (n = 3 independent biological specimens), adult stomach (n = 3 independent biological specimens), fetal stomach (n = 6 independent biological specimens), and fetal small intestine (n = 6 independent biological specimens) (see also Table S1). The top two principal components account for 68.3% of the variation in the data and show that HIOs group with adult and fetal tissues of the intestine, stomach, and colon, all of which are clearly distinct from endoderm and ESCs.

(legend continued on next page)

genes in the adult versus HIO comparison (Figure 1D). In addition, this comparison allowed us to identify genes uniquely upregulated in the adult versus HIO and in adult versus fetal comparisons. To further explore unique and common genes, we used the Gene Ontology Enrichment Analysis and Visualization (GOrilla) and Reduce and Visualize Gene Ontology (REVIGO) (Eden et al., 2007, 2009; Supek et al., 2011) discovery tools to examine biological processes that are enriched in each gene list (Figure 1E). GOrilla identifies significantly enriched gene ontology (GO) terms from a given gene list, and REVIGO then reduces redundancies by clustering semantically related terms and outputting them as a scatter plot for visualization. There were 240 significant GO terms identified by GOrilla from the list of 3,111 genes that were uniquely upregulated in adult versus HIO tissue. REVIGO reduced these to 72 unique GO terms (Figure 1E, left; Table S4). For the 2,287 genes uniquely upregulated in adult versus fetal intestine, there were 68 significant GO terms identified by GOrilla, which were reduced to 24 unique GO terms in REVIGO (Figure 1E, right; Table S5). Impressively, there were 609 significant GO terms identified from the list of 2,719 overlapping genes (Figure 1E, middle; Table S6). The list of GO terms enriched in the overlapping gene set was then reduced to 103 unique GO terms in REVIGO.

We chose to more closely examine biologically relevant GO terms identified by our analysis that were associated with the intestine (Table S6). To do so, we used fragments per kilobase of exon per million fragments mapped (FPKM) values generated from the RNA-seq dataset, and generated heatmaps for differentially expressed genes that fall under the GO terms "digestive tract development" (GO:0048565; Figure 1F) and "defense response" (GO:0006952; Figure 1G). Interestingly, the hierarchical clustering of the human adult and fetal samples with the HIO samples based solely on the genes contained within the GO category digestive tract development resulted in a dendrogram in which HIOs and fetal samples are intermingled, demonstrating the close relationship that HIOs share with fetal intestine with respect to this set of genes (Figure 1F). Some of the genes within the digestive tract development GO category that were highly expressed in both HIOs and fetal intestine included developmental signaling pathways important in fetal mouse intestine development, such as FGF and HH signaling (Nyeng et al., 2011; Walton et al., 2012).

A large number of genes involved in the defense response are highly expressed in adult intestine but expressed at low levels in both fetal tissue and HIOs (Figure 1G). These include genes involved in host defense against bacteria such as Paneth cell defensins (*DEFA5* and *DEFA6*) and genes for the intracellular bacterial-sensing NOD proteins. Upon examination of gene lists for differential expression (Tables S2 and S3), we also observed that expression of genes involved in digestion, Paneth cell function, and, most interestingly, the ISC marker *OLFM4* (van der Flier et al., 2009b; VanDussen et al., 2012) was markedly increased in the adult. We curated a heatmap to highlight a subset of genes involved in the

(B) A dendrogram was generated based on hierarchical clustering of the gene sets using Canberra distance. Fetal tissues are more similar to each other than to their respective adult tissues, and HIOs cluster within the same clade as the fetal tissues. Branch lengths indicate the level of dissimilarity between samples, with longer branch lengths indicating a greater level of dissimilarity. Red labels at branch point correspond to the approximately unbiased (AU) p value. AU > 95 indicates that a given branch assignment is strongly supported by the data. Green labels at each branch point correspond to the bootstrap probability (BP) of a cluster, defined as the frequency of a given relationship among the bootstrap replicates. ES, ESCs; HuSI, human small intestine; HuSI Duo, human small intestine duodenum; HuSI Dist, human distal small intestine; HuSto, human stomach.

(C) Spearman ranking was used to cluster samples and generate a heatmap of similarity, with dark red indicating the highest level of similarity between samples. The dendrogram indicates that HIOs are most similar to human small intestine.

(D) Differential gene expression analysis was carried out to identify genes that are upregulated in adult intestine compared to either HIOs (blue circle) or fetal intestine (yellow circle). The gene lists were then compared to determine how many genes overlap between those two comparisons (green), and the results are shown as a Venn diagram.

(E) The list of genes from each of the three categories of the Venn diagram were subjected to GO analysis to identify enriched GO terms. The results are shown as REVIGO (Supek et al., 2011) scatterplots in which similar GO terms are grouped in arbitrary two-dimensional space based on semantic similarity. Each circle indicates a specific GO term and circle sizes are indicative of how many genes are included in each term, where larger circles indicate a greater number of genes that are included in that GO term. Colors indicate the level of significance of enrichment of the GO term. Asterisks indicate terms that are hidden under other circles.

(F and G) Heatmaps were generated for gene sets belonging to the specific GO terms (F) Digestive Tract Development (GO:0048565) and (G) Defense Response (GO:0006952), and they further demonstrate that HIOs are more similar to fetal intestine with respect to these biological functions of the intestine.

(H) A curated heatmap was generated to examine particular genes that were chosen as being some of the most highly differentially expressed genes and were also of biological interest.

See also Figure S1.

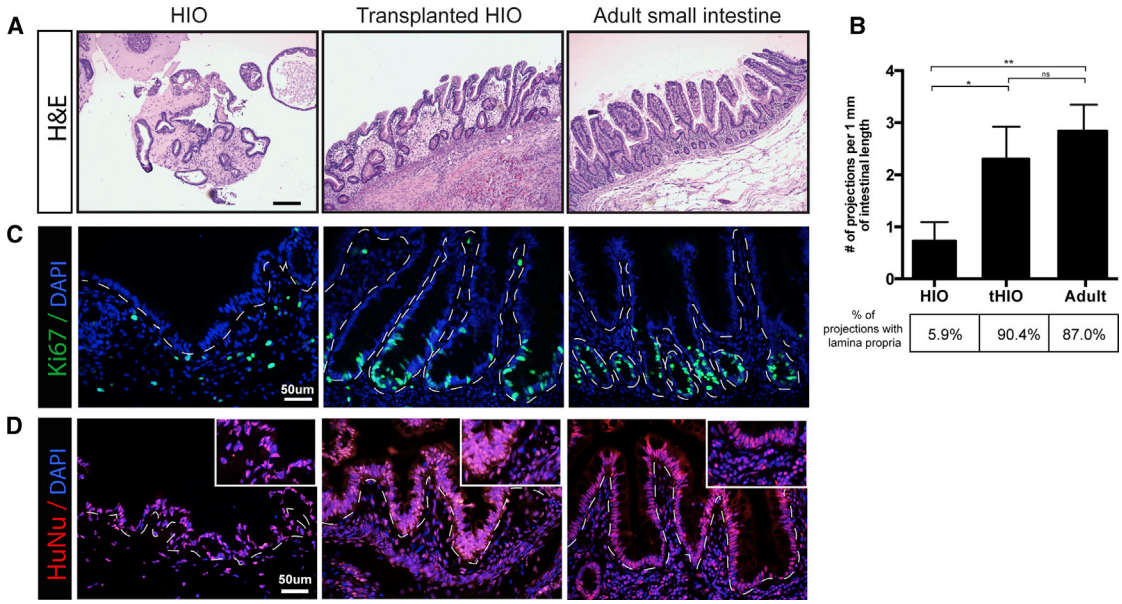

Figure 2. HIOs Develop Mature Architecture after In Vivo Transplantation

(A) H&E sections of an HIO, tHIO, and human intestine demonstrate that HIOs lack the characteristic crypt-villus units that are found in the adult small intestine and that transplanted HIOs (tHIOs) have a morphology that resembles the adult intestine.

(B) Villi morphology was quantified by counting the number of projections with a vimentin-positive core. tHIOs contain a similar number of villi per millimeter of intestinal length as adult intestine, whereas HIOs contain less projections and even fewer true villi. Three independently derived biological replicates for each tissue type with five fields of view for each sample were analyzed. Averages were compared using unpaired t tests. *p value 0.01–0.05, **p value 0.001–0.01.

(C) Ki67 staining demonstrates that the crypt-like domains are also the site of localized proliferation in both tHIOs and adult tissue.

(D) Staining for human nuclear antigen confirms that the tissue of intestinal morphology found in tHIOs is of human origin and not derived from the mouse host.

following: (1) digestive function, (2) Paneth cell function, (3) ISC regulation, and (4) expression in the lamina propria. Cumulatively, these data also demonstrated a strong correlation between HIO and fetal tissue compared to the adult (Figure 1H).

HIOs Develop Mature Architecture after In Vivo Transplantation

Previous work demonstrated that in vivo engraftment of HIOs into the kidney capsule of immunocompromised NSG (NOD-*scid* IL2Rgamma^{null}) mice (Ito et al., 2002) resulted in tissue with enhanced cellular differentiation and morphology (Watson et al., 2014). We sought to examine this further and determine if in vivo engraftment of HIOs would follow maturation into adult-like tissue based on predicted fetal-adult differences observed in the RNA-seq analysis (Figures 1F–1H). HIOs were grown in vitro for ~3 weeks and divided into two groups. One group was implanted under the kidney capsule of NSG mice; a matched control group was cultured in vitro only. Transplanted and control HIOs were compared after 16 weeks. Control HIOs that remained in vitro possessed epithelial thickenings that resembled villus-like domains, but generally lacked the crypt-villus architecture and underlying core of mesenchymal tissue (lamina propria) that typifies the human adult small intestine. However, transplanted HIOs (tHIOs) developed an architecture that more closely resembled the adult intestine with true villi containing a lamina propria (Figure 2A; Figure 6).

Projections resembling villi were counted and normalized per unit of length for HIO, tHIO, and adult intestine. Projections were categorized as villus-like, if they did not possess a lamina propria, or as true villi, if they possessed a lamina propria determined by the presence of vimentin staining within the center of the projection (Figure 3). The percentage of projections that were true villi for each condition was determined (Figure 2B). HIOs contained less than one projection per millimeter of epithelial length and only 5.6% of them could be classified as villi. In comparison, tHIO and adult intestine had two to three projections per millimeter of epithelium, of which 90.4% and 87% were true villi with a lamina propria, respectively (Figure 2B). Furthermore, proliferation was localized to the crypt-like domains in tHIOs as indicated by Ki67 staining

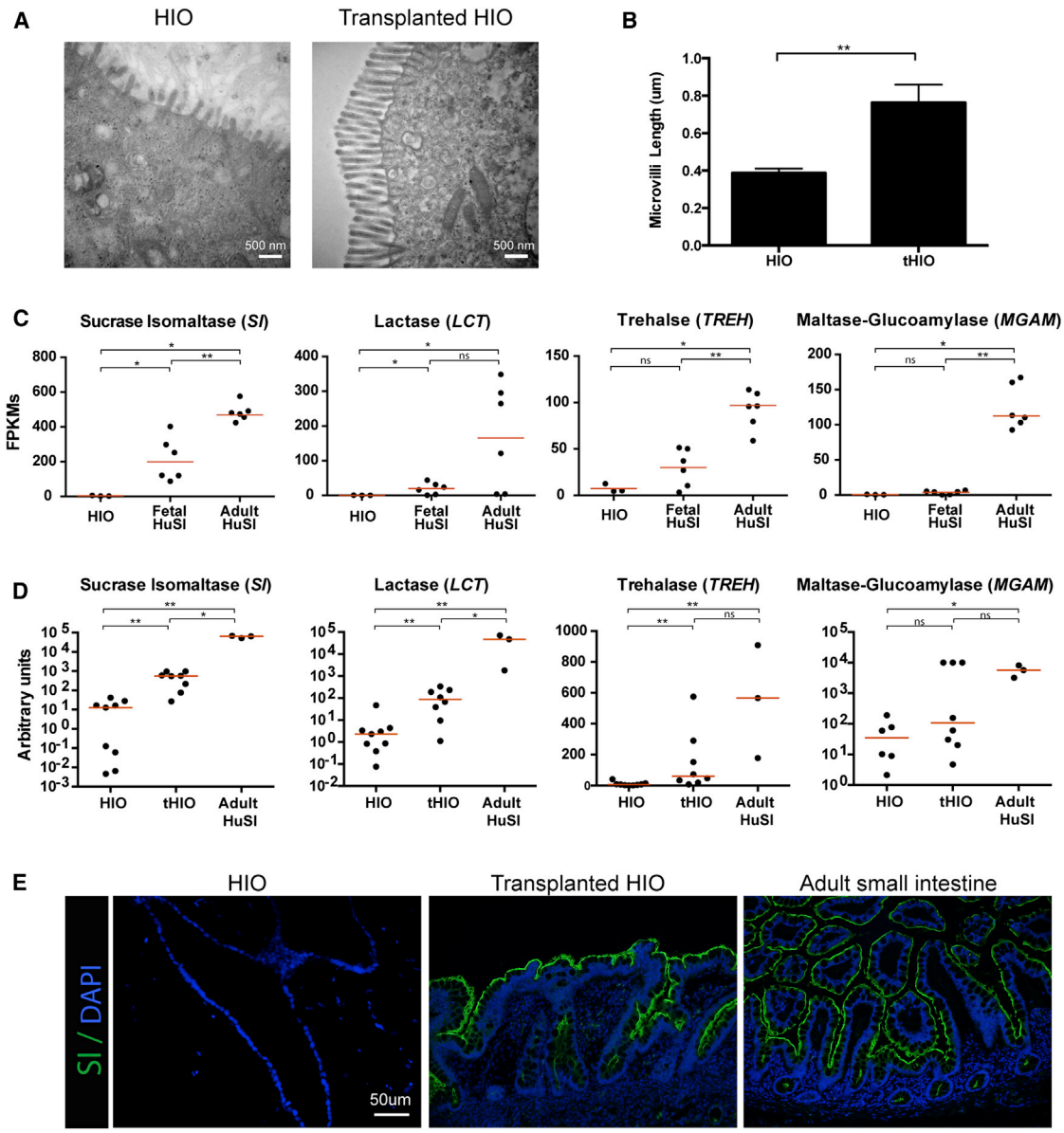

Figure 3. HIOs Express Brush Border Enzymes after In Vivo Transplantation

(A) HIOs have sparse and short microvilli compared to the microvilli present in tHIO cells, as determined by electron microscopy.

(B) Quantification of microvilli length indicates tHIOs have microvilli that are approximately two times longer than microvilli on HIO cells. Six independently derived HIOs and six tHIOs were analyzed with five measurements taken per sample. Averages were compared using unpaired t tests. **p value 0.001–0.01.

(C) Normalized FPKMs were plotted for HIOs (n = 3 independently differentiated from H9s), fetal small intestine (n = 6 independent biological specimens), and adult small intestine (n = 6 independent biological specimens), with each sample represented by a black dot. Red bars indicate the average FPKM value for each group. Brush border enzymes involved in carbohydrate digestion are expressed at low levels in both HIOs and fetal intestine, whereas they are highly expressed in adult intestine. *p value 0.01–0.05, **p value 0.001–0.01, ***p value 0.0001–0.001. All samples are biological replicates.

(D) Transplantation of HIOs into the kidney capsule results in an increase in the expression of brush border enzymes. qRT-PCR analysis was carried out by normalizing gene expression to the housekeeping gene *GAPDH* and plotting values as a.u. (n = at least 3 biological replicates for each tissue).

(E) Immunofluorescence shows that sucrase isomaltase protein expression is not detectable in HIOs, but is evident in tHIOs and resembles the expression seen in adult intestine.

See also Figures S2 and S3.

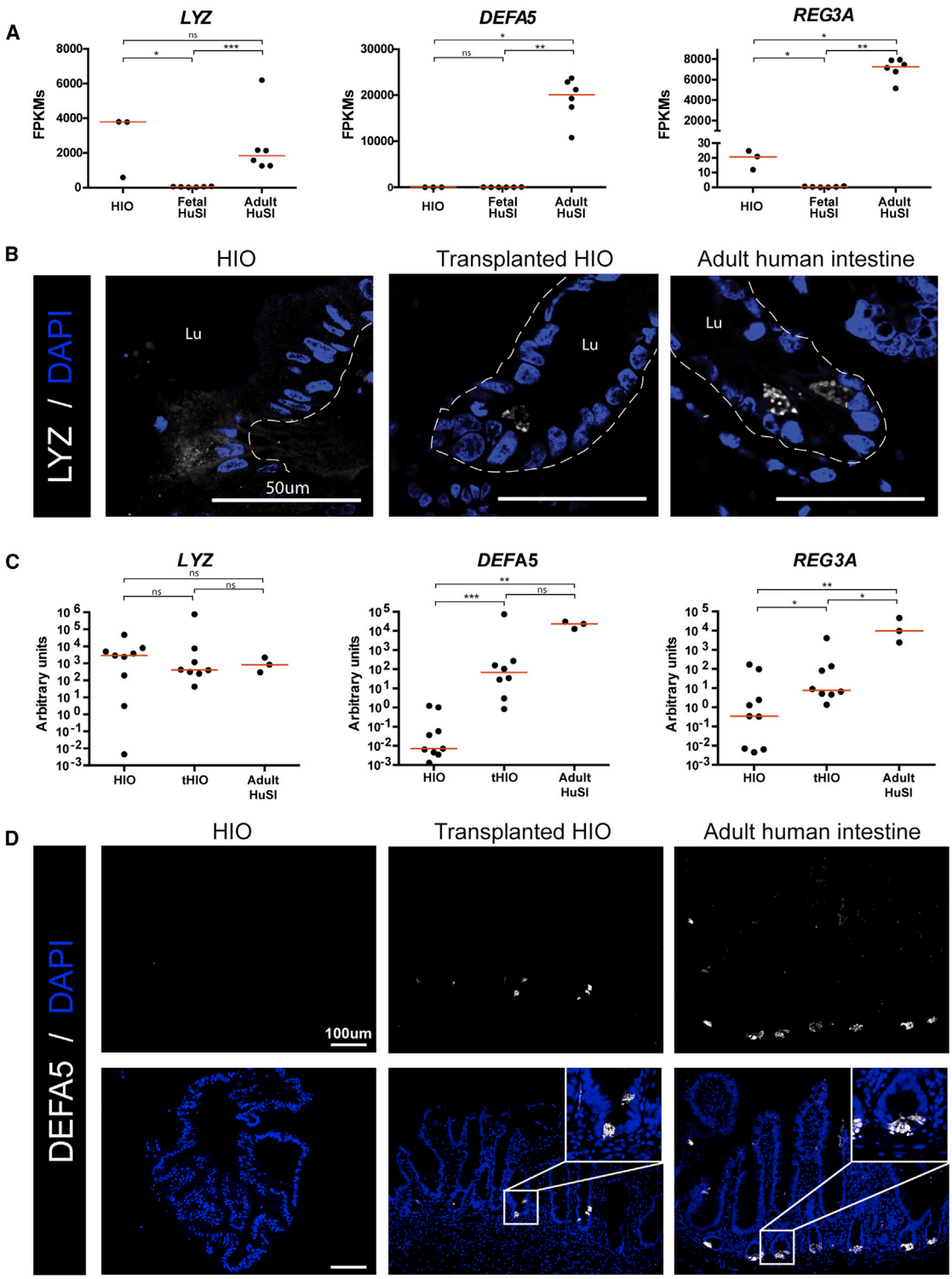

Figure 4. HIOs Form Crypts In Vivo Containing Mature Paneth Cells

(A) Normalized FPKMs were plotted for HIOs (n = 3 independently derived H9-HIOs), fetal small intestine (n = 6 independent biological specimens), and adult small intestine (n = 6 independent biological specimens), with each sample represented by a black dot. Red bars indicate the average FPKM value for each group. Lysozyme (*LYZ*) is expressed in HIOs at a similar level to adult intestine; however, mature

(legend continued on next page)

(Figure 2C). Staining for human nuclear antigen confirmed that the transplanted intestinal tissues were of human origin and therefore derived from transplanted HIOs (Figure 2D).

HIOs Have Enhanced Brush Border Enzyme Expression after In Vivo Transplantation

HIOs possess the predominant epithelial cell types of the small intestine that are present in both fetal and adult human intestine (Figure 3; Figure S2; Spence et al., 2011). Enterocytes of the small intestine are apically lined with microvilli, which are referred to as the brush border of the intestine. Transmission electron microscopy analysis and comparison of HIOs to tHIOs revealed that the brush border in HIOs is not as well developed (Figure 3A); tHIOs have microvilli that are nearly twice as long as the microvilli present in HIOs (Figure 3B). These findings are consistent with previous reports in which the microvilli in the fetal intestine were reported to be an average of 1 μm in length by 8 weeks of gestation and grow in length from 9–10 weeks of gestation through 15 weeks of gestation (Kelley, 1973; Moxey and Trier, 1979). Studies in the adult have shown that jejunal microvilli range from 0.67 to 1.3 μm in length (Brown and Badylak, 2014), with duodenal microvilli being slightly shorter than jejunal microvilli (Helander and Fändriks, 2014). Consistent with microvilli function, our transcriptome-wide analysis suggested that many critical functional enzymes are expressed at low levels in HIOs and fetal tissue compared to adult (Figures 1G and 3C). For example, FPKM values for the brush border enzymes sucrase isomaltase (*SI*), trehalase (*TREH*), lactase (*LCT*), and maltase glucoamylase (*MGAM*) demonstrated that expression of these genes was lowest in HIOs and highest in adult intestine (Figure 3C).

To demonstrate that the changes we saw in expression of brush border enzymes were not due to variations in the tissue collected for RNA-seq, we examined expression of multiple epithelial genes (Figure S3A). Through this analysis, we found that there were no consistent trends in epithelial-specific gene expression between any of the samples, suggesting that there were no underlying differences in the samples that could skew our interpretations. For example, there was no consistent evidence to suggest that certain samples had an over-representation of epithelial gene expression compared to the others. This data provided confidence that gene expression differences are reflective of true biological differences.

To determine if brush-border-related gene expression in tHIOs resembles adult tissue, we examined RNA expression of a number of genes by qRT-PCR. Expression in HIOs, tHIOs, and adult intestine was determined and is shown as arbitrary units of expression. We confirmed by qRT-PCR that tHIOs had enhanced expression of many genes, including *SI*, *LCT*, and *FABP2*, relative to HIOs (Figure 3D; Figure S1B). This adult-like pattern of gene expression in the tHIOs was not universally applicable, as some genes, including *TREH*, *MGAM*, and *MEP1B* (Figure 3D; Figure S3B), did not show robust induction after transplantation. Immunofluorescence staining confirmed that tHIOs appeared indistinguishable from adult small intestine in the expression of the brush border enzyme SI, whereas SI was undetectable in control HIOs (Figure 3E).

Paneth Cell Differentiation Is a Hallmark of Intestinal Maturation

Paneth cells play many important roles in the small intestine, acting as a niche for ISCs (Sato et al., 2011b) and secreting a variety of host-defense molecules including antimicrobial peptides (Clevers and Bevins, 2013). Lysozyme (LYZ), an enzyme that destroys the cell wall of bacteria, was the first host-defense product identified in Paneth cells (Deckx et al., 1967; Peeters and Vantrappen, 1975). RNA-seq data confirmed our previous findings (Spence et al., 2011) that *LYZ* is expressed in HIOs and also demonstrated that the human fetal intestine expresses low levels of *LYZ* compared to adult intestine (Figure 4A). *LYZ* expression was variable in HIOs and therefore was not significantly different from either fetal or adult intestine (Figure 4A). Our analysis suggested that HIOs do not possess fully differentiated Paneth cells since other Paneth cell genes/protein had low expression, including *DEFA5* (Mallow et al., 1996) and *REG3A* (Clevers and Bevins, 2013), similar to fetal tissue (Figures 1F and 4A). These results were consistent with previous data showing that *DEFA5* expression is low in the fetal intestine and increases as the intestine matures (Mallow et al., 1996).

Paneth cell markers *DEFA5* and *REG3A* are both expressed at high levels in adult intestine and expressed at very low levels in both HIO and fetal intestine. *p value 0.01–0.05, **p value 0.001–0.01, ***p value 0.0001–0.001. All samples are biological replicates.

(B) Immunofluorescence staining shows that lysozyme is diffusely expressed in HIOs, but is localized to punctate granules in transplanted HIOs and adult intestine.

(C) Transplantation of HIOs (tHIOs) into the kidney capsule results in an increase in expression of Paneth cell genes. qRT-PCR analysis was carried out by normalizing gene expression to the housekeeping gene *GAPDH* and plotting values as a.u. (n = at least 3 biologically independently differentiated HIOs and tHIOs, or independent biological intestinal specimens).

(D) Immunofluorescence staining shows that α-defensin 5 is not detectable in HIOs, but shows a similar staining pattern in both tHIOs and adult intestine.

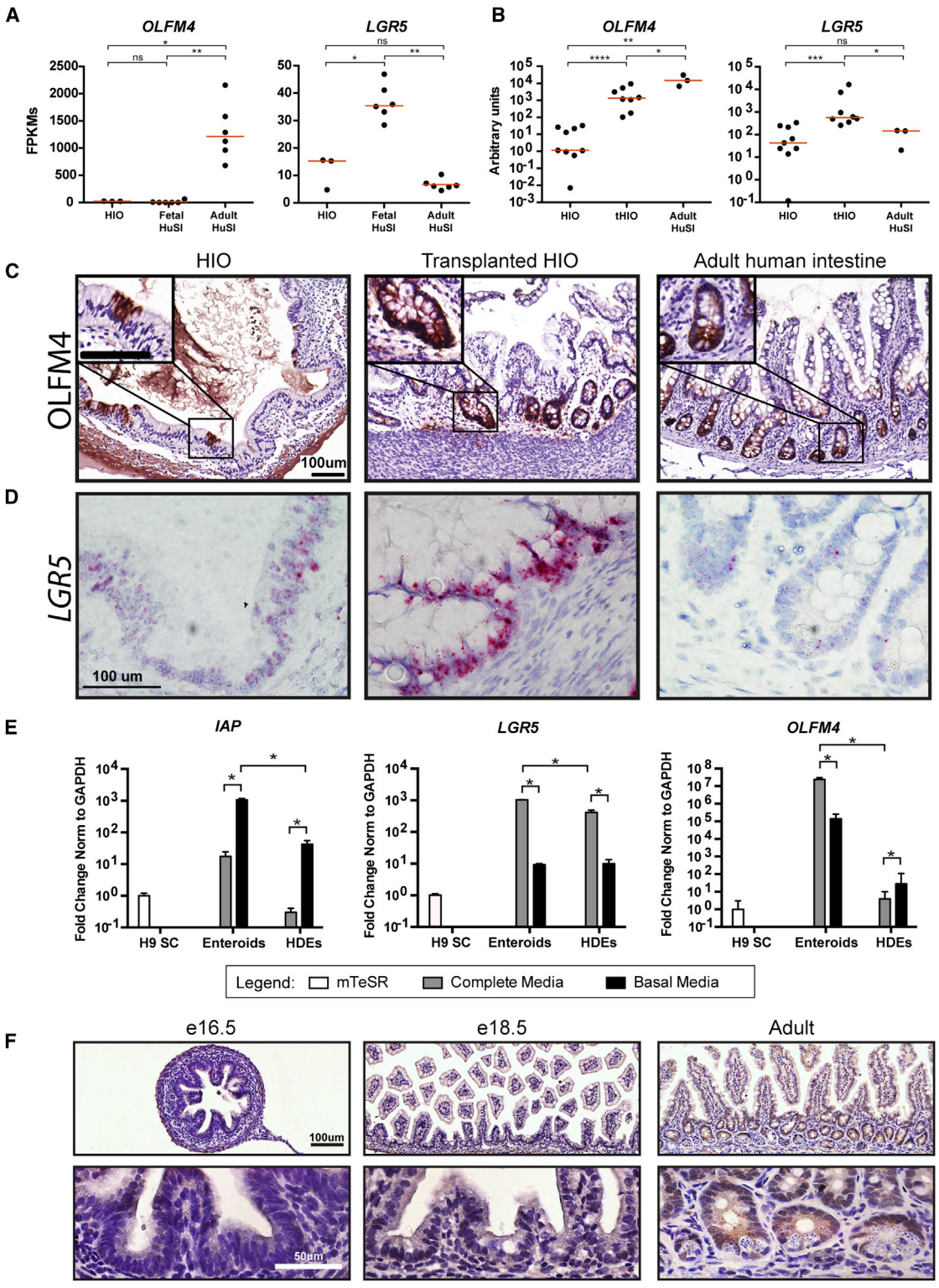

Figure 5. OLFM4 Is a Marker of Mature Intestine

(A) Normalized FPKMs were plotted for HIOs (n = 3 independently differentiated from H9s), fetal small intestine (n = 6 independent biological specimens), and adult small intestine (n = 6 independent biological specimens), with each sample represented by a black dot. Red bars indicate the average FPKM value for each group. *LGR5* is expressed to a similar level in both HIOs and adult human intestine;

(legend continued on next page)

Given that Paneth cells reside in the intestinal crypts and that Paneth cell genes were different between HIOs/fetal and adult intestine, we wanted to determine if tHIOs exhibited enhanced Paneth cell gene expression and localization to crypt-like domains. One of the hallmarks of mature Paneth cells is the packaging of antimicrobial peptides and LYZ into secretory granules. Consistent with our previous findings and with reports of LYZ expression in the fetal mouse intestine (Spence et al., 2011), LYZ protein expression was found as diffuse cytoplasmic staining in HIOs; the appearance of distinct secretory granules was not obvious (Figure 4B). This is in contrast to the strong granular lysozyme staining observed in Paneth cells of the adult intestine and tHIOs (Figure 4B). We also examined mRNA expression for *DEFA5* and *REG3A* in HIOs, tHIOs, and adult tissue. High expression of *DEFA5* and *REG3A* was observed in tHIOs, similar to adult intestine and distinct from HIOs (Figure 4C). Consistent with qRT-PCR data, protein expression of α-defensin 5 was not detected by immunofluorescence in HIOs, but was present in granular structures in the crypt-like domains of tHIOs and the crypts of the adult intestine (Figure 4D). Collectively, these results suggest that HIOs contained immature cells that diffusely expressed lysozyme but lacked other antimicrobial peptides. Furthermore, transplantation of HIOs into the murine kidney capsule resulted in Paneth cells that resembled those found in the adult human intestine.

OLFM4 Is a Marker of Mature Intestine

Our results demonstrate that the significant differences in Paneth cell maturity between HIO/fetal intestine and tHIO/adult intestine also were correlated with robust developmental changes in the well-characterized stem cell gene *OLFM4* (van der Flier et al., 2009b; VanDussen et al., 2012; Figure 1). We observed low *OLFM4* transcript abundance in the HIOs and fetal intestine RNA-seq datasets relative to the adult intestine, which exhibited ~69- and 108-fold higher expression, respectively (Figure 5A). In contrast, *LGR5* was expressed in all tissues examined and showed the most robust expression in the human fetal intestine (Figure 5A), which is consistent with other reports of high LGR5 expression in human fetal small intestine (Fordham et al., 2013). We recently showed robust LGR5 expression in LGR5:eGFP HIOs and tHIOs (Watson et al., 2014) and confirmed this by in situ hybridization (Figure 5D; Figure S5), suggesting that the observed changes in *OLFM4* are a unique developmental event. Thus, we further investigated OLFM4 gene and protein expression within HIOs, tHIOs, and adult intestine (Figures 5B and 5C). qRT-PCR analysis demonstrated an increase in *OLFM4* expression after HIO transplantation that was comparable to expression in the adult intestine (Figure 5B). At the protein level, OLFM4 was expressed in HIOs in small patches of epithelial cells that were sporadically distributed throughout the epithelium of the organoid. In serial section analysis, OLFM4+ patches were not common and were not localized to any obvious morphological structures (Figure 5C; data not shown). In contrast, OLFM4 expression was regularly observed and spatially restricted to crypt-like domains in tHIOs in the same manner as observed in the adult intestine.

Many reports have demonstrated OLFM4 to be a reliable marker of LGR5+ crypt base columnar (CBC) stem cells in the adult small intestine (Schuijers et al., 2014; van der Flier et al., 2009a). To further probe the stem cell populations in HIOs, we compared HIOs to adult human

however, there is higher expression detected in human fetal intestine. In contrast, *OLFM4* is expressed at a very low level in both HIOs and fetal intestine, but is dramatically higher in adult intestine. All samples are biological replicates.

(B) *OLFM4* expression is enhanced in tHIOs and is similar to the level of expression in adult intestine, whereas the level of expression in HIOs is much lower. qRT-PCR analysis was carried out by normalizing gene expression to the housekeeping gene *GAPDH* and plotting values as a.u. (n = at least 3 biological replicates for each tissue).

(C) Immunohistochemistry demonstrates that HIOs do express OLFM4 protein; however, OLFM4 is sporadically expressed throughout HIOs and cannot be detected in all histological sections. After transplantation, OLFM4 is readily detectable in all histological sections, and it is localized to crypt-like domains in a pattern similar to adult human intestine.

(D) In situ hybridization confirms that tHIOs express a higher level of *LGR5* and that HIOs express a level similar to adult intestine.

(E) Epithelium-only cultures were used to functionally analyze the responsiveness of enterocyte and stem cell gene expression to changes in culture conditions. Mature human enteroids express a higher level of *IAP* than immature HDEs when grown in complete media, which favors stem cells (gray bars, left). An increase in *IAP* expression in basal media for both enteroids and HDEs confirms that removal of pro-stem cell factors results in increased differentiation as expected (black bars, left). *LGR5* is expressed to similar levels in both enteroids and HDEs grown in complete media (gray bars, middle). In contrast, *OLFM4* is highly expressed in enteroids, but is barely detected in HDEs (gray bars, right). Growth of both enteroids and HDEs in basal media results in a reduction of *LGR5* expression (black bars, middle); however, *OLFM4* expression is only reduced in enteroids, but not HDEs grown in basal media (black bars, right). n = 3 biological replicates for all tissues. *p value 0.01–0.05.

(F) To confirm the developmental pattern of OLFM4 seen in human tissues, we also examined histological sections of mouse intestine at different developmental ages. OLFM4 was only detected in the adult intestine and not at any of the embryonic ages examined.

See also Figures S4 and S5.

crypt-derived enteroids (Sato et al., 2011a) in functional experiments. Importantly, enteroids are epithelium-only structures. Therefore, to carry out fair comparisons between the two systems, we used gentle enzymatic digestion and mechanical disruption to remove the mesenchymal cell population from HIOs, and we grew the epithelium from HIOs in the same human complete media used to grow enteroids (Figure S4; Table S7). The resulting epithelium contained structures that morphologically resembled human enteroids and are referred to as HIO-derived epithelium (HDE).

To examine the functional response of stem cells in enteroids and HDEs, we carried out a straightforward media-swapping experiment. Enteroids or HDEs were grown in human complete media for 7 days and subsequently either maintained in complete media, which promotes stem cell maintenance, or switched to basal media lacking small molecules and growth factors for an additional 7 days (Table S7). We predicted that complete media would promote maintenance of stem cells and expression of *LGR5* and *OLFM4* in human enteroids, whereas basal media would result in a reduction of stem cell gene expression and an increase in differentiated cell markers. qRT-PCR expression of intestinal alkaline phosphatase (*IAP*), which is expressed by mature enterocytes (Hinnebusch et al., 2004), was below the level of detection in HDEs (based on undifferentiated H9 human ESCs as a reference), though it could be detected in enteroids grown in complete media (Figure 5E, gray bars). As predicted, upon switching to basal media, a significant induction of *IAP* occurred in both HDE and enteroids (Figure 5E, gray versus black bars). Under standard culture conditions in complete media, *LGR5* was statistically higher in enteroids than HDEs albeit only modestly so (Figure 5E, gray bars). As predicted, in both enteroids and HDEs, basal media conditions led to reduced expression of *LGR5*. In contrast to *LGR5*, *OLFM4* was robustly expressed in enteroids and was barely detectable in HDEs. Moreover, basal media conditions led to a significant reduction of *OLFM4* only in adult enteroids (Figure 5E, gray versus black bars).

To corroborate our findings from HIOs and human tissue, we also examined OLFM4 protein expression at different stages of mouse development using immunohistochemistry. OLFM4 protein could not be detected at any of the fetal time points that we examined, but was present in the crypts in histological sections of adult mouse intestine (Figure 5F). These results are supported by microarray studies by others showing a robust increase in *OLFM4* gene expression from postnatal day (p)4 to p30 (Schjoldager et al., 2008; GEO profile 45876166). Collectively, our results suggest that acquisition of strong expression of OLFM4 in adult ISCs is a hallmark of the maturation process in humans and mice.

HIO Mesenchymal Cell Populations Gain Adult-like Organization after Transplantation

Given the emergence of villi in tHIOs (Figure 2B), we also wanted to examine cell types found in the lamina propria of the intestine to see how they compare between fetal and adult tissues, and in HIOs, tHIOs, and adult tissue. Based on our RNA-seq analysis, expression of mesenchymal markers vimentin (*VIM*) and smooth muscle actin (*ACTG2*) were not statistically different between fetal and adult intestines (Figure 6A). PDGFR-α-positive mesenchymal clusters have been demonstrated to direct the emergence of villi in mice (Walton et al., 2012). Consistent with this notion, *PDGFRA* expression was statistically higher in fetal intestine compared to adult intestine. All three markers were detectable at the protein level and were expressed throughout the mesenchyme of HIOs (Figure 6B). After transplantation, however, the organization of the mesenchymal cells resembled that seen in adult intestine, most notably for smooth muscle actin (SMA) and PDGFRA. A prominent band of organized SMA+ smooth muscle was present beneath the epithelium of both tHIOs and adult intestine. Likewise, PDGFRA+ cells lined the basal side of the epithelial cells of the villi in both tHIOs and adult intestine, whereas PDGFRA+ cells were spread throughout HIOs.

DISCUSSION

We examined gene expression in human intestinal tissue across the developmental continuum in order to determine maturity of in-vitro-derived HIOs. Using global RNA expression data obtained by RNA-seq, several different analyses demonstrated that the HIO transcriptome closely resembles global gene expression in the human fetal intestine, strongly suggesting that HIOs more accurately represent fetal intestinal tissue than adult intestinal tissue. The adult intestine is a complex organ that performs many important metabolic and immunologic functions and hosts a tremendous population of indigenous bacteria. Our RNA-seq analysis supports the existing body of literature demonstrating that the human fetal intestine is immature with respect to advanced metabolic and host-defense functions, and that acquisition of these features is a hallmark of maturation to adult function. Similar to the human fetal gut, we have demonstrated that HIOs lack strong expression of many digestion-related genes and Paneth cells. We have further demonstrated that HIOs are competent to acquire these attributes of the adult intestine. This process requires transplantation into an in vivo context, suggesting that our in vitro conditions lack important cues for maturation. We suspect that cues from multiple sources are required to induce full maturation. For example, animal studies have

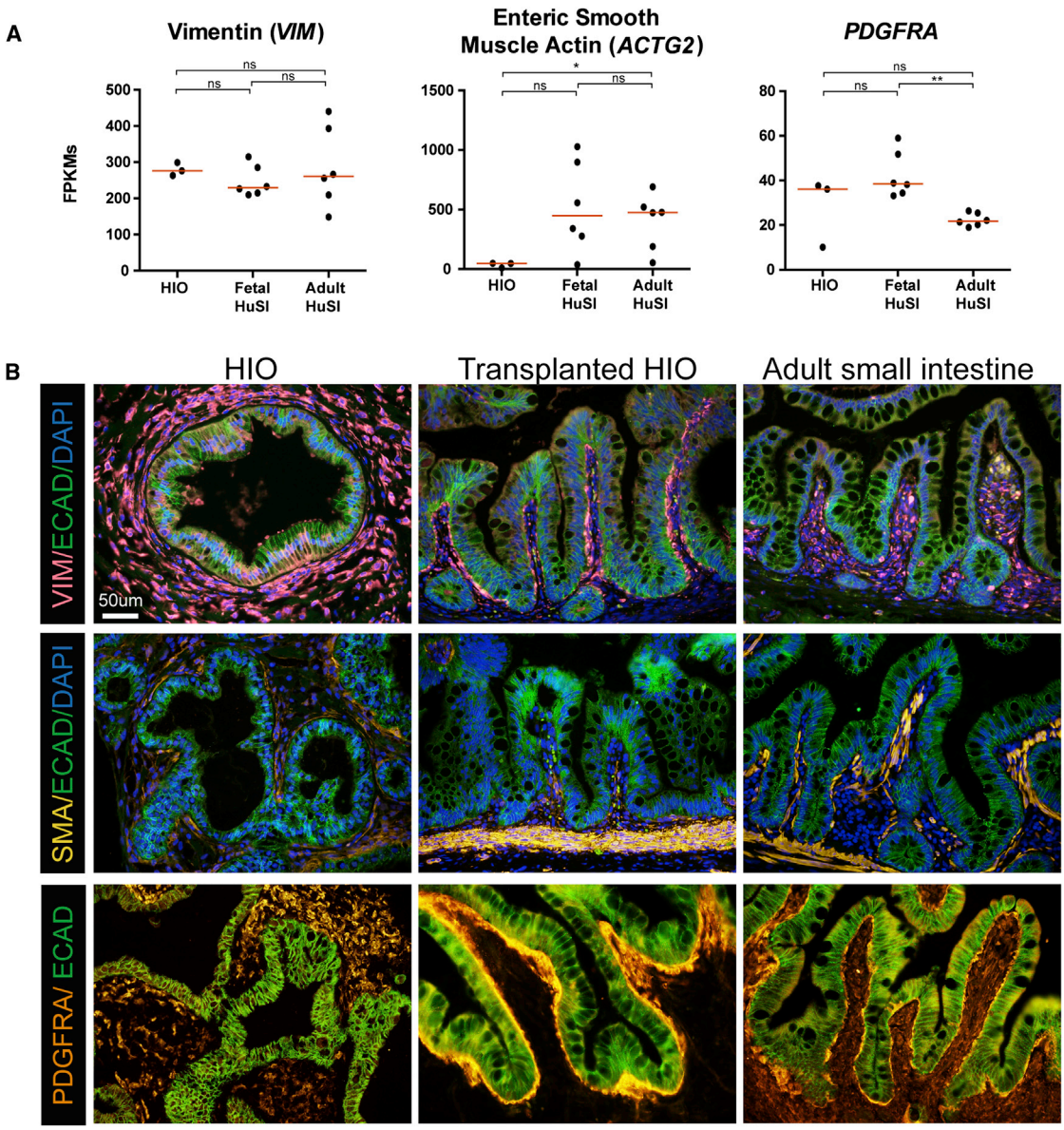

Figure 6. HIOs Express Mesenchymal Cell Markers but Become Organized Like Adult Intestine after Transplantation

(A) Normalized FPKMs were plotted for HIOs (n = 3 independently differentiated from H9s), fetal small intestine (n = 6 independent biological specimens), and adult small intestine (n = 6 independent biological specimens), with each sample represented by a black dot. Red bars indicate the average FPKM value for each group. *VIM* is expressed to a similar level across HIOs and fetal and adult human intestines. HIOs express lower levels of *ACTG2* than adult tissue, with fetal tissue expressing a range of levels. Most of the HIO and fetal intestine samples express a higher level of *PDGFRa* than adult tissue.

(B) The expression trends are confirmed by immunofluorescence staining with most notable changes in the spatial arrangement of positive cells for all three markers. All samples are biological replicates with an n. *p value 0.01–0.05, **p value 0.001–0.01, ***p value 0.0001–0.001.

highlighted the importance of intestinal microbial colonization in enhancing intestinal function, development of the intestinal immune system, and protection against pathogenic infection (Cash et al., 2006; Hooper, 2004; Hooper et al., 1999, 2001, 2012; Hudault et al., 2001). Moreover, it was recently demonstrated that HIOs transplanted into the kidney capsule could respond to circulating factors (Watson et al., 2014).

Our finding that OLFM4 is not highly expressed in human or mouse fetal intestine but marks ISCs in the

adult intestine is intriguing and suggests that there may be significant differences between fetal and adult ISCs. Importantly, the two predominant pathways that regulate adult ISCs, Wnt and Notch, are both thought to be important in late fetal development in mice (Korinek et al., 1998; Tsai et al., 2014; VanDussen et al., 2012; Zhong et al., 2012). Thus, it is possible that acquisition of an adult ISC state occurs gradually across the developmental continuum, such that there are differences in ISC regulation in early fetal development, late fetal development, postnatally, and in adult life. At this time, careful studies across different developmental ages have not been carried out. It is also currently unclear if the gene expression differences between fetal and adult life are functionally significant because, for example, Olfm4 knockout animals do not show a phenotype (Schuijers et al., 2014).

In addition to HIOs, other groups have established primary cell culture models of the human and mouse fetal intestine, called fetal enterospheres (Fordham et al., 2013; Mustata et al., 2013). Mouse fetal enterospheres only retain fetal properties for a limited time because they continue to develop into adult-like organoids. Therefore, it appears as though the developmental program may be hardwired into the epithelium that is removed from the fetal gut, and may pose limitations to the use of primary fetal tissue. While fetal enterospheres are an invaluable tool, our results show that HIOs offer a complementary system that may be more accessible to a wider portion of the research community. Given the difficulty or inability to obtain human fetal tissue for many researchers, in addition to the ethical and legal concerns of using this tissue in biomedical research, our data suggest that HIOs provide an appropriate alternative model.

Taken together, our results show that HIOs represent the fetal/immature intestine, and we have identified several hallmarks of fetal-to-adult intestine development that can be modeled in HIOs transplanted into mice. Given the limitations in acquiring human fetal tissue and the even greater limitations of performing functional experiments on this tissue, HIOs provide unique opportunities to explore human fetal intestinal biology. Importantly, we also have demonstrated that discoveries made using HIOs are recapitulated during fetal development and adult maturation in mice, highlighting the power of this system to make important discoveries.

EXPERIMENTAL PROCEDURES

Generation of HIOs

HIOs were generated as previously described (McCracken et al., 2011; Spence et al., 2011; Xue et al., 2013). For details, see the Supplemental Experimental Procedures.

Human Tissue

Human adult small intestinal tissue was collected from deceased donors through the Gift of Life, Michigan. Institutional review board (IRB) approval was obtained for use of human tissues (University of Michigan IRB HUM00024263). Segments of the small intestine were collected, and mucosal scrapings were used to generate enteroids or collected and snap frozen for RNA analysis. Whole-thickness tissue was fixed and embedded in paraffin or cryomold protectant (O.C.T., Fisherbrand) for histological purposes. HIOs were collected in the same manner.

Growth of Adult Human Enteroids

Human enteroids were isolated as previously described (Miyoshi et al., 2012). Enteroids were propagated in complete media as described in Table S7. Conditioned media were generated from Wnt3a-expressing L cells (ATCC CRL-2647) and R-spondin 2-expressing cells (Bell et al., 2008). Biological replicates of enteroids consisted of ~15–20 enteroids per replicate.

RNA-Seq and Analysis

RNA was extracted using the Trizol extraction protocol from the manufacturer (Life Technologies). Library preparation and sequencing of HIOs was performed in the University of Michigan DNA Sequencing Core on the Illumina Hi-Seq 2000 platform using TruSeq library preparations. The Bioinformatics Core at the University of Michigan processed all RNA-seq data. See the Supplemental Experimental Procedures for a detailed description of methods and for details regarding informatics analysis. All data and analyses are available online (https://github.com/hilldr/Finkbeiner_StemCellReports2015).

Kidney Capsule Implants

As previously described (Watson et al., 2014), HIOs that had been in culture for ~3 weeks were removed from matrigel and embedded into purified type I collagen (BD Biosciences) and allowed to form a solid plug before being placed back into standard growth media overnight. NSG mice (NOD-*scid* IL2Rgamma^{null}) (Ito et al., 2002) were used for the implants. All animal work was reviewed and approved by institutional animal care and use committees.

qRT-PCR, Histology, and Microscopy

The qRT-PCR, histology, immunostaining, and microscopy were essentially carried out as previously described (Rockich et al., 2013; Spence et al., 2009, 2011). For additional details, see the Supplemental Experimental Procedures.

Statistical Analyses

Data are expressed as the median of each sample set with each data point represented in the plots. Fetal samples from different post-conception days were treated as one group, available adult small intestinal samples were treated as another, and then HIO and tHIOs were treated as their own groups. Unless otherwise noted in the figure legend, pairwise comparisons were carried out as indicated with GraphPad Prism 5.0 software using unpaired Mann-Whitney t tests due to the non-normal distribution of the data. Significant values are denoted as

follows: *p value 0.01–0.05, **p value 0.001–0.01, and ***p value 0.0001–0.001. At least three biological replicates for each group were used in all experiments.

ACCESSION NUMBERS

The accession number for all sequences reported in this paper is EMBL-EBI ArrayExpress: E-MTAB-3158.

SUPPLEMENTAL INFORMATION

Supplemental Information includes Supplemental Experimental Procedures, five figures, and nine tables and can be found with this article online at http://dx.doi.org/10.1016/j.stemcr.2015.04.010.

AUTHOR CONTRIBUTIONS

S.R.F. and J.R.S. conceived the study. S.R.F., D.R.H., M.J.T., P.H.D., Y.-H.T., A.M.C., C.H.A., M.M.M., C.L.W., and J.J.F. conducted experiments. S.R.F., D.R.H., M.J.T., P.H.D., Y.-H.T., P.J.D., and J.R.S. analyzed results. R.N., M.T., M.M.M., O.D.K., N.F.S., M.A.H., D.H.T., and P.J.D. provided critical material support. S.R.F. and J.R.S. wrote the manuscript. All authors read and edited the manuscript and approved the final contents.

ACKNOWLEDGMENTS

We thank Rich McEachin and Manjusha Pande at the University of Michigan Bioinformatics Core Facility. We also thank the Gift of Life, Michigan, for access to human intestinal tissue. This work was supported by grants from the National Institute of Diabetes and Digestive and Kidney Diseases (NIDDK, K01DK091415 and U01DK103141) to J.R.S. and by the University of Michigan Center for Gastrointestinal Research (UMCGR) (NIDDK, 5P30DK034933). Research reported in this publication and conducted by S.R.F. was supported by an NIDDK training grant, "Training in Basic and Translational Digestive Sciences" (T32DK094775), a postdoctoral fellowship from The Hartwell Foundation, and the National Center for Advancing Translational Sciences of the NIH (2UL1TR000433). Additionally, this work was supported by a grant from the California Institute for Regenerative Medicine (RN3-06525) to O.D.K. The content is solely the responsibility of the authors and does not necessarily represent the official views of the NIH.

Received: December 16, 2014
Revised: April 22, 2015
Accepted: April 22, 2015
Published: June 4, 2015

REFERENCES

Bell, S.M., Schreiner, C.M., Wert, S.E., Mucenski, M.L., Scott, W.J., and Whitsett, J.A. (2008). R-spondin 2 is required for normal laryngeal-tracheal, lung and limb morphogenesis. Development *135*, 1049–1058.

Brown, B.N., and Badylak, S.F. (2014). Extracellular matrix as an inductive scaffold for functional tissue reconstruction. Transl. Res. *163*, 268–285.

Cash, H.L., Whitham, C.V., Behrendt, C.L., and Hooper, L.V. (2006). Symbiotic bacteria direct expression of an intestinal bactericidal lectin. Science *313*, 1126–1130.

Chen, Y.-J., Finkbeiner, S.R., Weinblatt, D., Emmett, M.J., Tameire, F., Yousefi, M., Yang, C., Maehr, R., Zhou, Q., Shemer, R., et al. (2014). De novo formation of insulin-producing "neo-β cell islets" from intestinal crypts. Cell Rep. *6*, 1046–1058.

Clevers, H.C., and Bevins, C.L. (2013). Paneth cells: maestros of the small intestinal crypts. Annu. Rev. Physiol. *75*, 289–311.

Deckx, R.J., Vantrappen, G.R., and Parein, M.M. (1967). Localization of lysozyme activity in a Paneth cell granule fraction. Biochim. Biophys. Acta *139*, 204–207.

Du, A., McCracken, K.W., Walp, E.R., Terry, N.A., Klein, T.J., Han, A., Wells, J.M., and May, C.L. (2012). Arx is required for normal enteroendocrine cell development in mice and humans. Dev. Biol. *365*, 175–188.

Dye, B.R., Hill, D.R., Ferguson, M.A., Tsai, Y.-H., Nagy, M.S., Dyal, R., Wells, J.M., Mayhew, C.N., Nattiv, R., Klein, O.D., et al. (2015). In vitro generation of human pluripotent stem cell derived lung organoids. eLife *4*, e05098.

Eden, E., Lipson, D., Yogev, S., and Yakhini, Z. (2007). Discovering motifs in ranked lists of DNA sequences. PLoS Comput. Biol. *3*, e39.

Eden, E., Navon, R., Steinfeld, I., Lipson, D., and Yakhini, Z. (2009). GOrilla: a tool for discovery and visualization of enriched GO terms in ranked gene lists. BMC Bioinformatics *10*, 48.

Finkbeiner, S.R., and Spence, J.R. (2013). A gutsy task: generating intestinal tissue from human pluripotent stem cells. Dig. Dis. Sci. *58*, 1176–1184.

Finkbeiner, S.R., Zeng, X.-L., Utama, B., Atmar, R.L., Shroyer, N.F., and Estes, M.K. (2012). Stem cell-derived human intestinal organoids as an infection model for rotaviruses. MBio *3*, e00159.

Fordham, R.P., Yui, S., Hannan, N.R.F., Soendergaard, C., Madgwick, A., Schweiger, P.J., Nielsen, O.H., Vallier, L., Pedersen, R.A., Nakamura, T., et al. (2013). Transplantation of expanded fetal intestinal progenitors contributes to colon regeneration after injury. Cell Stem Cell *13*, 734–744.

Helander, H.F., and Fändriks, L. (2014). Surface area of the digestive tract - revisited. Scand. J. Gastroenterol. *49*, 681–689.

Hinnebusch, B.F., Siddique, A., Henderson, J.W., Malo, M.S., Zhang, W., Athaide, C.P., Abedrapo, M.A., Chen, X., Yang, V.W., and Hodin, R.A. (2004). Enterocyte differentiation marker intestinal alkaline phosphatase is a target gene of the gut-enriched Kruppel-like factor. Am. J. Physiol. Gastrointest. Liver Physiol. *286*, G23–G30.

Hooper, L.V. (2004). Bacterial contributions to mammalian gut development. Trends Microbiol. *12*, 129–134.

Hooper, L.V., Xu, J., Falk, P.G., Midtvedt, T., and Gordon, J.I. (1999). A molecular sensor that allows a gut commensal to control its nutrient foundation in a competitive ecosystem. Proc. Natl. Acad. Sci. USA *96*, 9833–9838.

Hooper, L.V., Wong, M.H., Thelin, A., Hansson, L., Falk, P.G., and Gordon, J.I. (2001). Molecular analysis of commensal host-microbial relationships in the intestine. Science *291*, 881–884.

Hooper, L.V., Littman, D.R., and Macpherson, A.J. (2012). Interactions between the microbiota and the immune system. Science *336*, 1268–1273.

Hrvatin, S., O'Donnell, C.W., Deng, F., Millman, J.R., Pagliuca, F.W., DiIorio, P., Rezania, A., Gifford, D.K., and Melton, D.A. (2014). Differentiated human stem cells resemble fetal, not adult, β cells. Proc. Natl. Acad. Sci. USA *111*, 3038–3043.

Hudault, S., Guignot, J., and Servin, A.L. (2001). Escherichia coli strains colonising the gastrointestinal tract protect germfree mice against Salmonella typhimurium infection. Gut *49*, 47–55.

Ito, M., Hiramatsu, H., Kobayashi, K., Suzue, K., Kawahata, M., Hioki, K., Ueyama, Y., Koyanagi, Y., Sugamura, K., Tsuji, K., et al. (2002). NOD/SCID/gamma(c)(null) mouse: an excellent recipient mouse model for engraftment of human cells. Blood *100*, 3175–3182.

Kelley, R.O. (1973). An ultrastructural and cytochemical study of developing small intestine in man. J. Embryol. Exp. Morphol. *29*, 411–430.

Korinek, V., Barker, N., Moerer, P., van Donselaar, E., Huls, G., Peters, P.J., and Clevers, H. (1998). Depletion of epithelial stem-cell compartments in the small intestine of mice lacking Tcf-4. Nat. Genet. *19*, 379–383.

Leslie, J.L., Huang, S., Opp, J.S., Nagy, M.S., Kobayashi, M., Young, V.B., and Spence, J.R. (2015). Persistence and toxin production by Clostridium difficile within human intestinal organoids result in disruption of epithelial paracellular barrier function. Infect. Immun. *83*, 138–145.

Li, X., Udager, A.M., Hu, C., Qiao, X.T., Richards, N., and Gumucio, D.L. (2009). Dynamic patterning at the pylorus: formation of an epithelial intestine-stomach boundary in late fetal life. Dev. Dyn. *238*, 3205–3217.

Mallow, E.B., Harris, A., Salzman, N., Russell, J.P., DeBerardinis, R.J., Ruchelli, E., and Bevins, C.L. (1996). Human enteric defensins. Gene structure and developmental expression. J. Biol. Chem. *271*, 4038–4045.

McCracken, K.W., Howell, J.C., Wells, J.M., and Spence, J.R. (2011). Generating human intestinal tissue from pluripotent stem cells in vitro. Nat. Protoc. *6*, 1920–1928.

Miyoshi, H., Ajima, R., Luo, C.T., Yamaguchi, T.P., and Stappenbeck, T.S. (2012). Wnt5a potentiates TGF-β signaling to promote colonic crypt regeneration after tissue injury. Science *338*, 108–113.

Moxey, P.C., and Trier, J.S. (1979). Development of villus absorptive cells in the human fetal small intestine: a morphological and morphometric study. Anat. Rec. *195*, 463–482.

Mustata, R.C., Vasile, G., Fernandez-Vallone, V., Strollo, S., Lefort, A., Libert, F., Monteyne, D., Pérez-Morga, D., Vassart, G., and Garcia, M.-I. (2013). Identification of Lgr5-independent spheroid-generating progenitors of the mouse fetal intestinal epithelium. Cell Rep. *5*, 421–432.

Nyeng, P., Bjerke, M.A., Norgaard, G.A., Qu, X., Kobberup, S., and Jensen, J. (2011). Fibroblast growth factor 10 represses premature cell differentiation during establishment of the intestinal progenitor niche. Dev. Biol. *349*, 20–34.

Peeters, T., and Vantrappen, G. (1975). The Paneth cell: a source of intestinal lysozyme. Gut *16*, 553–558.

Rockich, B.E., Hrycaj, S.M., Shih, H.P., Nagy, M.S., Ferguson, M.A.H., Kopp, J.L., Sander, M., Wellik, D.M., and Spence, J.R. (2013). Sox9 plays multiple roles in the lung epithelium during branching morphogenesis. Proc. Natl. Acad. Sci. USA *110*, E4456–E4464.

Sato, T., Stange, D.E., Ferrante, M., Vries, R.G.J., Van Es, J.H., Van den Brink, S., Van Houdt, W.J., Pronk, A., Van Gorp, J., Siersema, P.D., and Clevers, H. (2011a). Long-term expansion of epithelial organoids from human colon, adenoma, adenocarcinoma, and Barrett's epithelium. Gastroenterology *141*, 1762–1772.

Sato, T., van Es, J.H., Snippert, H.J., Stange, D.E., Vries, R.G., van den Born, M., Barker, N., Shroyer, N.F., van de Wetering, M., and Clevers, H. (2011b). Paneth cells constitute the niche for Lgr5 stem cells in intestinal crypts. Nature *469*, 415–418.

Schjoldager, K.T.B.G., Maltesen, H.R., Balmer, S., Lund, L.R., Claesson, M.H., Sjöström, H., Troelsen, J.T., and Olsen, J. (2008). Cellular cross talk in the small intestinal mucosa: postnatal lymphocytic immigration elicits a specific epithelial transcriptional response. Am. J. Physiol. Gastrointest. Liver Physiol. *294*, G1335–G1343.

Schuijers, J., van der Flier, L.G., van Es, J., and Clevers, H. (2014). Robust cre-mediated recombination in small intestinal stem cells utilizing the olfm4 locus. Stem Cell Reports *3*, 234–241.

Spence, J.R., Lange, A.W., Lin, S.-C.J., Kaestner, K.H., Lowy, A.M., Kim, I., Whitsett, J.A., and Wells, J.M. (2009). Sox17 regulates organ lineage segregation of ventral foregut progenitor cells. Dev. Cell *17*, 62–74.

Spence, J.R., Mayhew, C.N., Rankin, S.A., Kuhar, M.F., Vallance, J.E., Tolle, K., Hoskins, E.E., Kalinichenko, V.V., Wells, S.I., Zorn, A.M., et al. (2011). Directed differentiation of human pluripotent stem cells into intestinal tissue in vitro. Nature *470*, 105–109.

Supek, F., Bošnjak, M., Škunca, N., and Šmuc, T. (2011). REVIGO summarizes and visualizes long lists of gene ontology terms. PLoS ONE *6*, e21800.

Tsai, Y.-H., VanDussen, K.L., Sawey, E.T., Wade, A.W., Kasper, C., Rakshit, S., Bhatt, R.G., Stoeck, A., Maillard, I., Crawford, H.C., et al. (2014). ADAM10 regulates Notch function in intestinal stem cells of mice. Gastroenterology *147*, 822–834.

van der Flier, L.G., Haegebarth, A., Stange, D.E., van de Wetering, M., and Clevers, H. (2009a). OLFM4 is a robust marker for stem cells in human intestine and marks a subset of colorectal cancer cells. Gastroenterology *137*, 15–17.

van der Flier, L.G., van Gijn, M.E., Hatzis, P., Kujala, P., Haegebarth, A., Stange, D.E., Begthel, H., van den Born, M., Guryev, V., Oving, I., et al. (2009b). Transcription factor achaete scute-like 2 controls intestinal stem cell fate. Cell *136*, 903–912.

VanDussen, K.L., Carulli, A.J., Keeley, T.M., Patel, S.R., Puthoff, B.J., Magness, S.T., Tran, I.T., Maillard, I., Siebel, C., Kolterud, Å., et al. (2012). Notch signaling modulates proliferation and differentiation of intestinal crypt base columnar stem cells. Development *139*, 488–497.

Walton, K.D., Kolterud, A., Czerwinski, M.J., Bell, M.J., Prakash, A., Kushwaha, J., Grosse, A.S., Schnell, S., and Gumucio, D.L. (2012). Hedgehog-responsive mesenchymal clusters direct patterning

and emergence of intestinal villi. Proc. Natl. Acad. Sci. USA *109*, 15817–15822.

Watson, C.L., Mahe, M.M., Múnera, J., Howell, J.C., Sundaram, N., Poling, H.M., Schweitzer, J.I., Vallance, J.E., Mayhew, C.N., Sun, Y., et al. (2014). An in vivo model of human small intestine using pluripotent stem cells. Nat. Med. *20*, 1310–1314.

Wells, J.M., and Spence, J.R. (2014). How to make an intestine. Development *141*, 752–760.

Xue, X., Ramakrishnan, S., Anderson, E., Taylor, M., Zimmermann, E.M., Spence, J.R., Huang, S., Greenson, J.K., and Shah, Y.M. (2013). Endothelial PAS domain protein 1 activates the inflammatory response in the intestinal epithelium to promote colitis in mice. Gastroenterology *145*, 831–841.

Zhong, Z., Baker, J.J., Zylstra-Diegel, C.R., and Williams, B.O. (2012). Lrp5 and Lrp6 play compensatory roles in mouse intestinal development. J. Cell. Biochem. *113*, 31–38.

Stem Cell Reports, Volume *4*

Supplemental Information

Transcriptome-wide Analysis Reveals Hallmarks of Human Intestine Development and Maturation In Vitro and In Vivo

Stacy R. Finkbeiner, David R. Hill, Christopher H. Altheim, Priya H. Dedhia, Matthew J. Taylor, Yu-Hwai Tsai, Alana M. Chin, Maxime M. Mahe, Carey L. Watson, Jennifer J. Freeman, Roy Nattiv, Matthew Thomson, Ophir D. Klein, Noah F. Shroyer, Michael A. Helmrath, Daniel H. Teitelbaum, Peter J. Dempsey, and Jason R. Spence

Figure S1, related to Figure 1.

(A) Principal component analysis was conducted HIOs (n=3 independently derived H9-HIOs), adult distal small intestine (n=4 independent biological specimens), adult duodenum (n=2 independent biological specimens), and fetal small intestine (n=6 independent biological specimens) (see also Table S1). The top two principal components account for 76.8% of the variation in the data and show that HIOs group with fetal intestinal tissues. (B) A dendrogram was generated based on hierarchical clustering of the gene sets using Canberra distance (B). Fetal tissues are more similar to each other than to their respective adult tissues and HIOs cluster within the same clade as the fetal tissues. Branch lengths indicate the level of dissimilarity between samples, with longer branch lengths indicating a greater level of dissimilarity. Red labels at branch point correspond to the Approximately Unbiased (AU) p-value. AU > 95 indicates that a given branch assignment is strongly supported by the data. Green labels at each branch point correspond to the bootstrap probability (BP) of a cluster, defined as the frequency of a given relationship among the bootstrap replicates. HuSI=human small intestine, HuSI Dist=human distal small intestine, HuSI Duo=human duodenal small intestine. (C) Spearman ranking was used to cluster samples and generate a heatmap of similarity with dark red indicating the highest level of similarity between samples. The dendrogram indicates that HIOs are most similar to fetal small intestine.

Figure S2, related to Figure 3

HIOs, tHIOs, and adult intestine were stained for markers of differentiated intestinal cells. HIOs express DppIV, a marker of enterocytes, and this expression is maintained after transplantation. Expression resembles staining seen along the brush border of adult intestine.

The goblet cell marker Muc2 is expressed in HIOs and expression is maintained, if not increased, in tHIOs and resembles the staining seen in adult intestine. Lastly, enteroendocrine cells, marked by Chromogranin A (ChgA), are a relatively more rare cell type found in the adult intestine. This is also true in HIOs and tHIOs in which ChgA staining is detected sporadically throughout the tissues.

Figure S3, related to Figure 3

(A) Normalized FPKMs were plotted for HIOs (n=3 independently derived H9-HIOs), fetal small intestine (n=6 independent biological specimens), and adult small intestine (n=6 independent biological specimens). FPKM values show that epithelial specific gene expression does not follow any broad trend. This rules out significant sampling bias for any particular group of samples and justifies the comparison of epithelial gene expression between sample types. Each sample is represented by a single black dot and red bars indicate the average FPKM value for each group. *p-value: 0.01-0.05, **p-value: 0.01-0.001, ***p-value: 0.001-0.0001. (B) Fatty acid binding protein (*FABP*) expression is increased in tHIOs relative to HIOs and is expressed to nearly the same level as in adult intestine (left). Meprin A, beta (*MEP1B*) is an example of a digestion related gene that is not expressed at a higher level in tHIOs compared to HIOs. n=3 independently derived H9-tissues for HIOs and tHIOs. n=3 biologically independent adult intestine tissues. *p-value: 0.01-0.05, **p-value: 0.01-0.001, ***p-value: 0.001-0.0001.

Figure S4, related to Figure 5.

Epithelium was isolated from HIOs through enzymatic and mechanical isolation. Epithelium cultured in the standard media used for growth and maintenance of HIOs does not expand over time (left panel). In 'complete media', which is used to grow human enteroids, the epithelium grows as budding structures that resemble human enteroids (middle and right panel). The epithelial structures derived from HIOs are referred to as HIO-derived epithelium (HDEs).

Figure S5, related to Figure 5.
(A) Low magnification image of the LGR5 *in situ* hybridization from the same tissue as shown in Figure 5. LGR5 expression in adult intestine confirms the specificity of the LGR5 probe by showing it is restricted to the crypts. Scale bar = 100um. (B) A slightly higher magnification image that is zoomed in on a villus tip confirms there is no LGR5 signal present on the villus tip. Scale bar = 50um. (C) A slightly higher magnification image that is zoomed in on a crypt highlights the specificity of LGR5 signal to the base of the crypt. Scale bar = 50um.

Fig. S1, related to Figure 1

A.

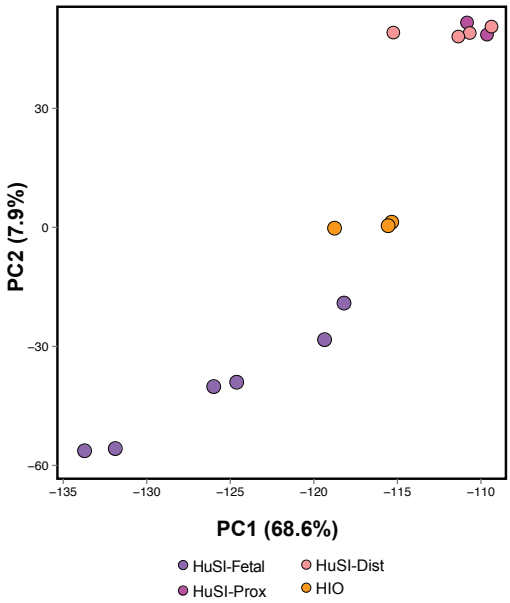

B.

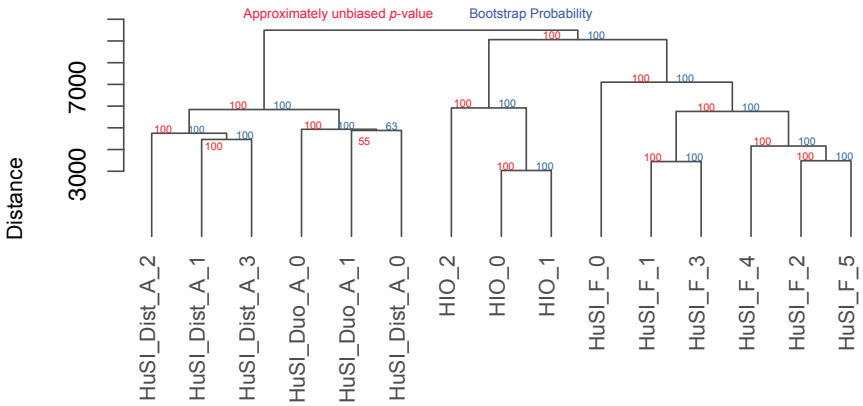

C.

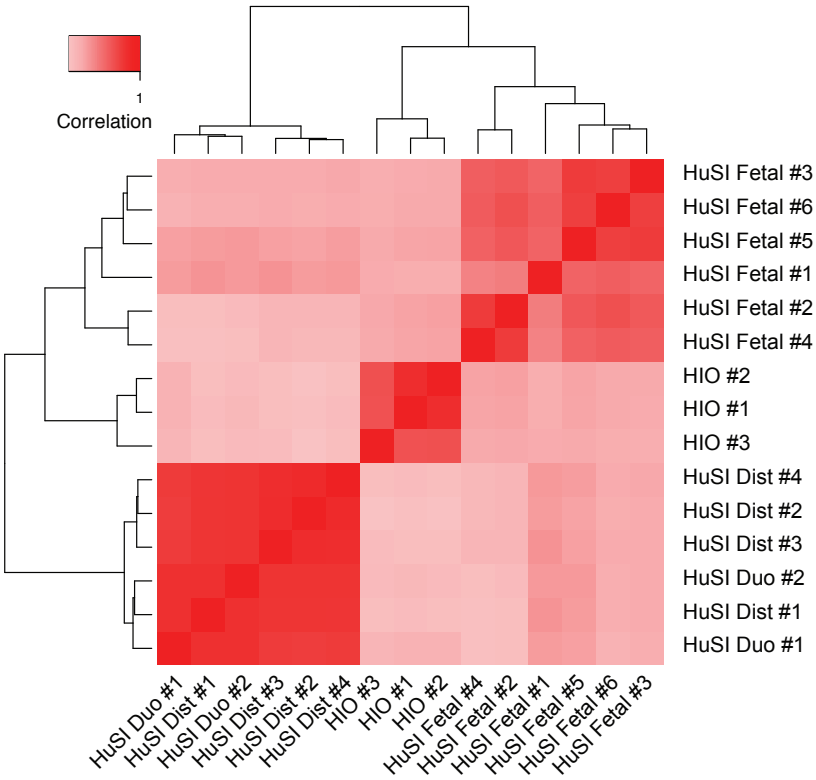

Figure S2, Related to Figure 3

A.

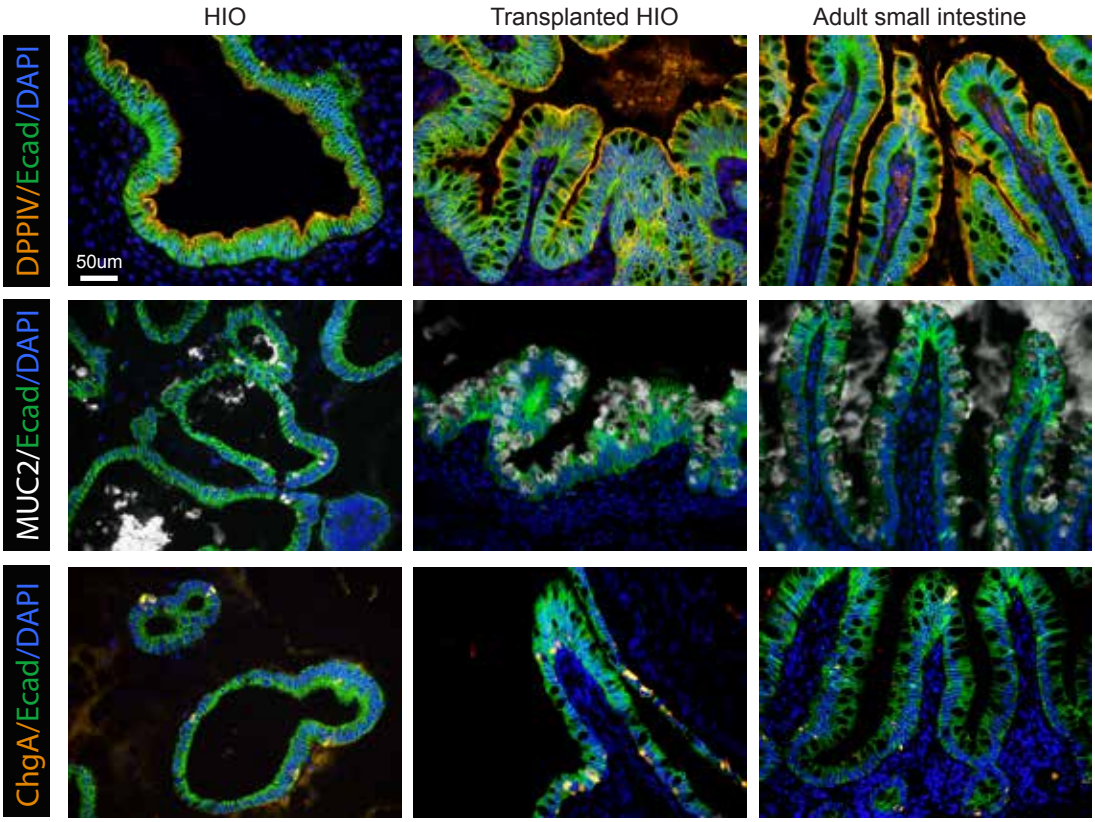

Figure Supplement 3- Related to Figure 3

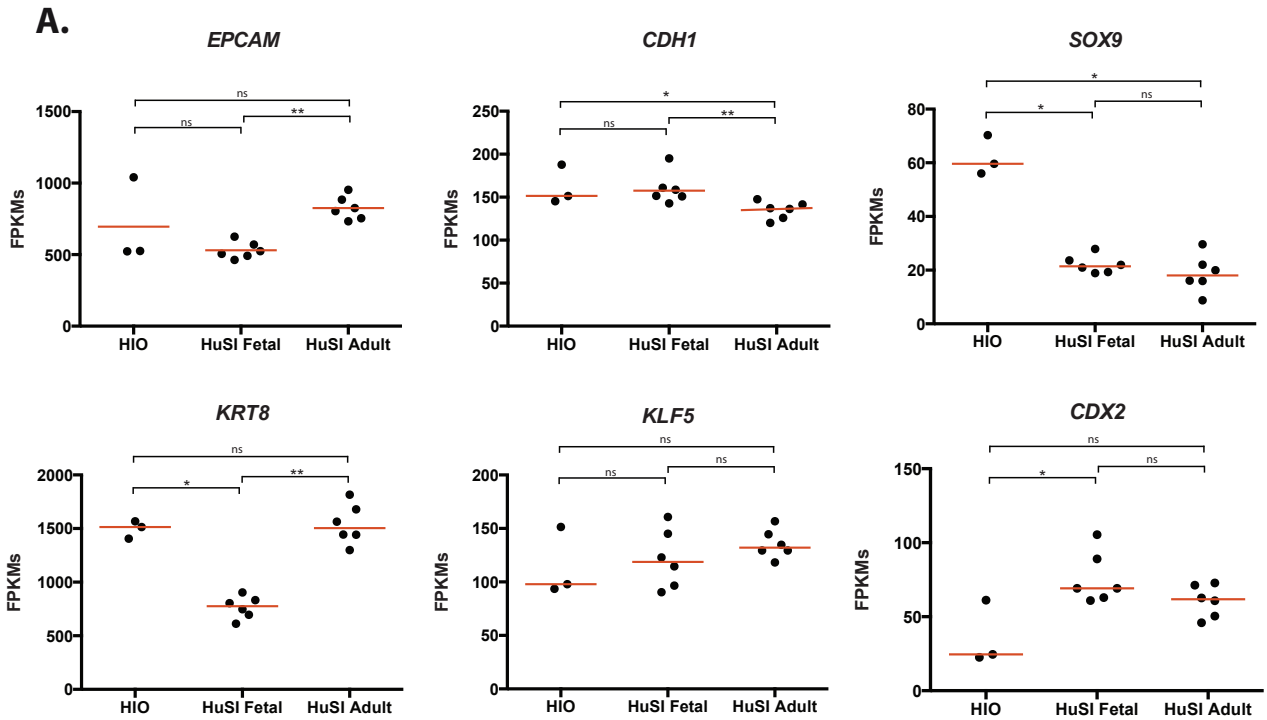

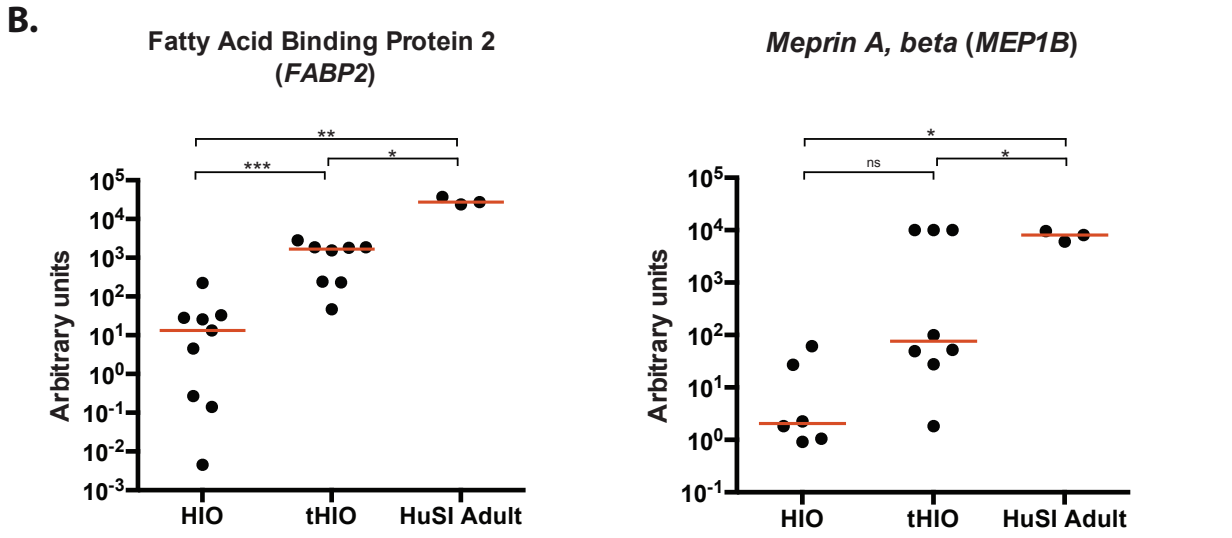

Figure S4 - Related to Figure 5

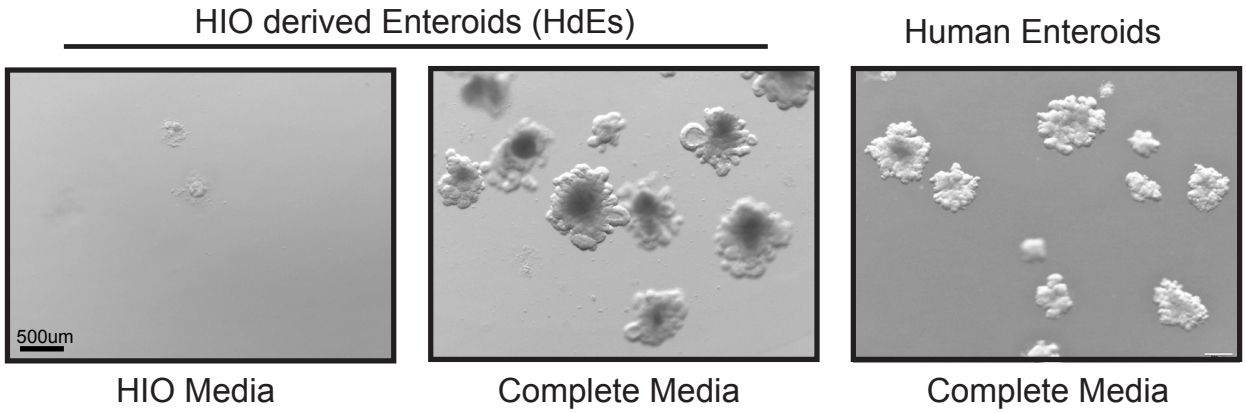

Figure S5, related to Figure 5

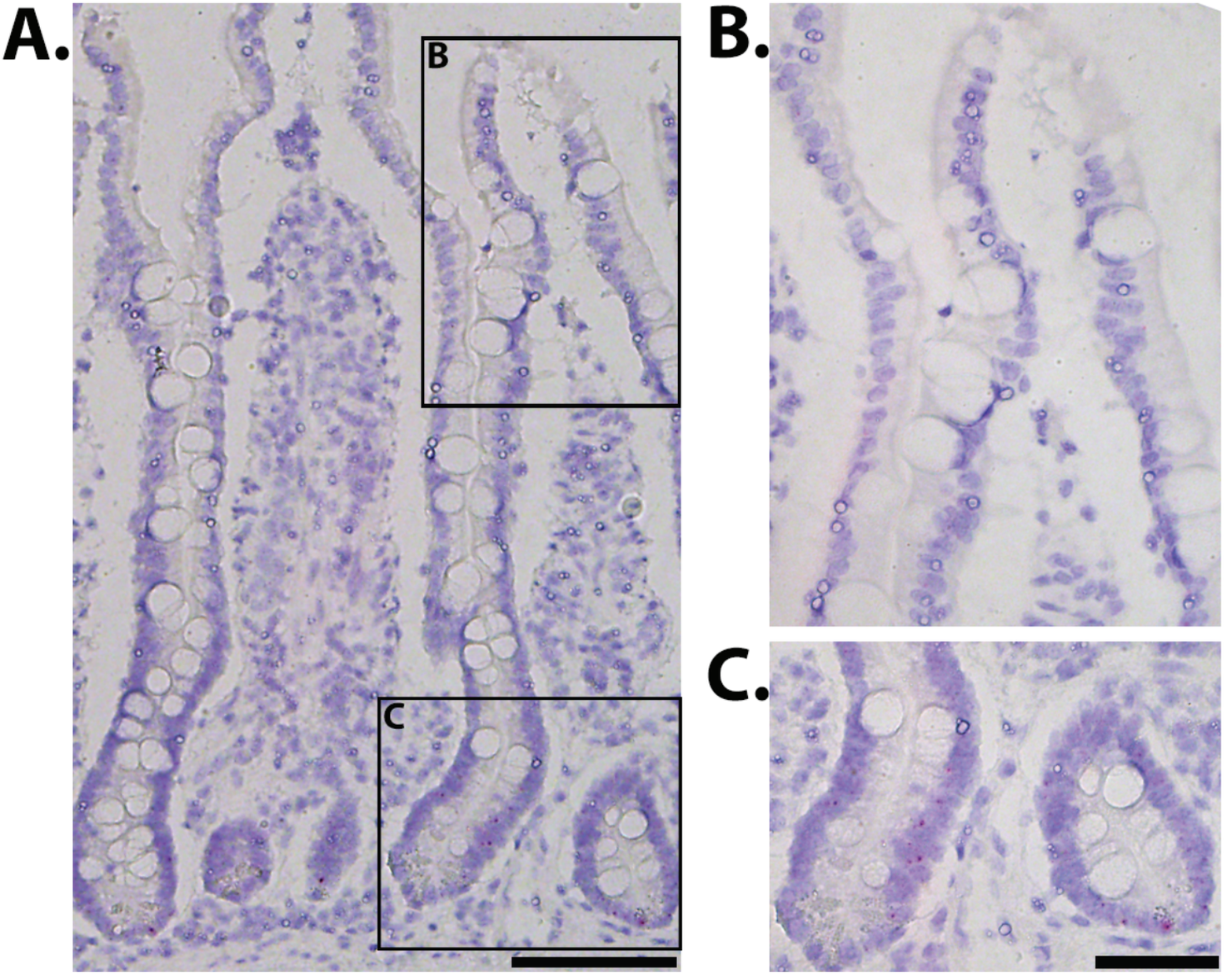

Table 1: RNAseq Datasets Downloaded from Public Databases

Sample Label	Description	Source	Donor ID	Accession #
HuSI.F91	Fetal Day 91, small intestine	GEO Datasets	H-23914	GSM1059508
HuSI.F98	Fetal Day 98, small intestine	GEO Datasets	H-23964	GSM1059521
HuSI.F108	Fetal Day 108, small intestine	GEO Datasets	H-23769	GSM1059486
HuSI.F108	Fetal Day 108, small intestine	GEO Datasets	H-23887	GSM1059507
HuSI.F115	Fetal Day 115, small intestine	GEO Datasets	H-23808	GSM1059517
HuSI.F120	Fetal Day 120, small intestine	GEO Datasets	H-23941	GSM1059519
HuSI.Duo.A1	Adult Duodenum	EMBL-EBI ArrayExpress	V145	E-MTAB-1733 (duodenum_4b)
HuSI.Duo.A2	Adult Duodenum	EMBL-EBI ArrayExpress	V150	E-MTAB-1733 (duodenum_4b)
HuSI.Dist.A1	Distal Small Intestine	EMBL-EBI ArrayExpress	V151	E-MTAB-1733 (small intestine_4a)
HuSI.Dist.A2	Distal Small Intestine	EMBL-EBI ArrayExpress	V152	E-MTAB-1733 (small intestine_4b)
HuSI.Dist.A3	Distal Small Intestine	EMBL-EBI ArrayExpress	V153	E-MTAB-1733 (small intestine_4c)
HuSI.Dist.A4	Distal Small Intestine	EMBL-EBI ArrayExpress	V156	E-MTAB-1733 (small intestine_4d)
HuStomach.F101	Fetal Day 101, stomach	GEO Datasets	H-24125	GSM1220600
HuStomach.F105	Fetal Day 105, stomach	GEO Datasets	H-24005	GSM1220597
HuStomach.F107	Fetal Day 107, stomach	GEO Datasets	H-23758	GSM1220590
HuStomach.F108	Fetal Day 108, stomach	GEO Datasets	H-23887	GSM1220587
HuStomach.F110	Fetal Day 110, stomach	GEO Datasets	H-23604	GSM1220589
HuStomach.F127	Fetal Day 127, stomach	GEO Datasets	H-24078	GSM1220598
HuStomach.A1	Adult stomach	EMBL-EBI ArrayExpress	V18	E-MTAB-1733 (stomach a)
HuStomach.A2	Adult stomach	EMBL-EBI ArrayExpress	V90	E-MTAB-1733 (stomach 3a)
HuStomach.A3	Adult stomach	EMBL-EBI ArrayExpress	V91	E-MTAB-1733 (stomach 3b)
HuColon.A1	Adult colon	EMBL-EBI ArrayExpress	V10	E-MTAB-1733 (colon a)
HuColon.A2	Adult colon	EMBL-EBI ArrayExpress	V11	E-MTAB-1733 (colon_b)
HuColan.A3	Adult colon	EMBL-EBI ArrayExpress	V14	E-MTAB-1733 (colon_c)

SI=small intestine, Dist=distal region of intestine, A=adult, F=fetal (numbers indicate days of gestation)

Table S7: Media Formulations for Enteroid Cultures, Related to Fig. 5

Reagent	Supplier	Catalog #	HIO Media	Complete Media	Basal Media
Advanced DMEM:F12	Life Technologies	12634	YES	YES	YES
B27 Supplement	Life	17504044	1X	1X	1X
N2 Supplement	Life Technologies		---	1X	1X
L-Glutamine	Life Technologies	25030	2mM	2mM	2mM
Pen-Strep	Life Technologies	15140	100/mL; 100ug/mL	100/mL; 100ug/mL	100/mL; 100ug/mL
HEPES	Life Technologies	15630080	15mM	15mM	15mM
EGF	R&D Systems	236-EG	100ng/mL	100ng/mL	100ng/mL
NOGGIN	R&D Systems	6057-NG	100ng/mL	100ng/mL	100ng/mL
R-Spondin 2 conditioned media	---	---	5%	25%	---
Chir99021	Tocris	4423	---	2.5uM	---
WNT3A conditioned media	---	---	---	25%	---
N-acetylcysteine	Sigma	A9165	---	2mM	---
Nicotinamide	Sigma	N0636	---	20mM	---
A-83-01	Tocris	2939	---	0.5 uM	---
SB202190	Sigma	S7067	---	2.5uM	---

Table S8: qRT-PCR Primers

Gene	Primer	Sequence
DEFA5	hDefA5-F	CCTTTGCAGGAAATGGACTC
	hDefA5-R	GGACTCACGGGTAGCACAAC
FABP2	hFABP2-F	GCTGCAAGCTTCCTTTTCAC
	hFABP2-R	CTGAAATCATGGCGTTTGAC
GAPDH	hGAPDH-F	CTCTGCTCCTCCTGTTCGAC
	hGAPDH-R	TTAAAAGCAGCCCTGGTGAC
IAP	hIAP-F	TCAGCTGGGTACTCAGGGTC
	hIAP-R	ATCGCCACTCAGCTCATCTC
LCT	hLCT-F	GGCAGTCTGGGAGTTTTAGG
	hLCT-R	ATGCCAAAATGAGGCAAGTC
LGR5	hLGR5-F	CAGCGTCTTCACCTCCTACC
	hLGF5-R	TGGGAATGTATGTCAGAGCG
LYZ	hLYZ-F	ACAAGCTACAGCATCAGCGA
	hLYZ-R	GTAATGATGGCAAAACCCCA
MEP1B	hMEP1B-F	AGATGGCCTCATACCATTCC
	hMEP1B-R	AGGCGATAACGTTCAAATGC
MGAM	hMGAM-F	GACATTGGCTGGGAGACAAC
	hMGAM-R	CTCCCGTATAGGATATGCCG
OLFM4	hOLFM4-F	ACCTTTCCCGTGGACAGAGT
	hOLFM4-R	TGGACATATTCCCTCACTTTGGA
REG3a	hReg3a-F	CTCCCTGGTGAAGAGCATTG
	hReg3a-R	TGCTACTCCACTCCCAACCT
SI	hSI-F	GGATGGTCACAGATGAAACCT
	hSI-R	TCCTCCCCATCGTCCACTA
TREH	hTREH-F	GGAGCTGTGCCTGCTACTG
	hTREH-R	CTCCCCGTGGCAGTAAATC

All primer sequences came from human qPCR Depot: http://primerdepot.nci.nih.gov/

Table S9: List of Antibodies Used

Antigen	Antibody Species	Company	Catalog #	Dilution
Alpha Defensin 5	mouse	Abcam	Ab90802	1:50
Human nuclear antigen	mouse	Millipore	MAB1281	1:100
Ki67	rabbit	ThermoScientific	RM-9106-S1	1:400
Lysozyme	goat	Santa Cruz	sc-27958	1:100
Olfm4	rabbit	Abcam	ab85046	1:100
Sucrase Isomaltase	goat	Santa Cruz	sc-27603	1:100
Vimentin	mouse	Sigma	V2258	1:200
Smooth muscle actin	mouse	Sigma	C6198	1:400
Pdgfra	rabbit	Santa Cruz	sc-338	1:100
Villin	goat	Santa Cruz	sc-7672	1:50
Mucin 2	rabbit	Santa Cruz	sc-15334	1:1000
Chromagranin A	goat	Santa Cruz	sc-1488	1:100

Supplemental Experimental Procedures

Generation of HIOs

Briefly, H9 embryonic stem cells were treated with Activin A (R&D Systems) for 3 days to generate endoderm. FGF4 (R&D Systems) and Chir99021 (STEMGENT), a Wnt agonist used in place of recombinant Wnt3a, were then used to pattern the endoderm into CDX2+ intestinal cells that spontaneously form floating, 3-dimensional aggregates called spheroids. Spheroids were collected and plated into droplets of Matrigel (BD Biosciences/Corning), a laminin-rich basement membrane complex. Spheroids were cultured in media containing EGF (100ng/mL, R&D Systems), R-Spondin 2 (5% conditioned media (Bell et al., 2008)), and Noggin (100ng/mL, R&D Systems) for 1 week and then in media containing only EGF and R-Spondin 2 thereafter as they grew into HIOs. HIOs used for experiments were grown *in vitro* for 1-2 months prior to use unless otherwise stated. Biological replicates of HIOs consist of pools of 5-8 HIOs per replicate.

RNA Sequencing

RNA sequencing data obtained from of three human intestinal organoid samples was appended to the normalized RNAseq data sets of 6 unique fetal intestinal tissue samples and 6 unique adult small intestinal tissue samples obtained from publicly available sources. The UM Bioinformatics Core concatenated sequence data from the UM sequencing core into a single. fastq file for each sample. Additional sequence data was retrieved from the EBI-AE database (Adult Samples) and NCBI-GEO (SRA) database (Fetal samples) (Table 1). The quality of raw reads for each sample were checked using FastQC (version 0.10.1) to identify features of the data that may indicate quality problems (e.g. low quality scores, over-represented sequences, inappropriate GC content, etc.). Adapter sequences were trimmed from the reads using Cutadapt (version 0.9.5) (Chen et al., 2014). The software package Tuxedo Suite was used for alignment, differential expression analysis, and post-analysis diagnostics (Langmead et al., 2009; Trapnell et al., 2009; 2013). Briefly, reads were aligned to the

reference transcriptome (UCSC hg19) (genome.ucsc.edu) using TopHat (version 2.0.9) and Bowtie (version 2.1.0.0). Default parameter settings were used for alignment, with the exception of allowing software to spend extra time searching for valid alignments and limiting the read mapping to known transcripts. In addition, we used FastQC for a second round of quality control (post-alignment), to ensure that only high quality data would be input to expression quantitation and differential expression analysis. Cufflinks/CuffDiff (version 2.1.1) was used for expression quantitation and differential expression analysis, using UCSC hg19.fa as the reference genome sequence and UCSC hg19.gtf as the reference transcriptome annotation. We used locally developed scripts to format and annotate the differential expression data output from CuffDiff. Briefly, we identified genes and transcripts as being differentially expressed based on three criteria: test status = “OK”, FDR < 0.05 and fold change ≥ 1.5. We annotated genes and isoforms with NCBI Entrez GeneIDs and text descriptions. We further annotated differentially expressed genes with Gene Ontology (GO) (www.geneontology.org) terms using NCBI annotation.

Gene ontology analysis and heatmaps

Biological process gene ontology categories with putative roles in intestinal development were identified using the Gene Ontology Consortium database (Ashburner et al., 2000). Genbank gene symbols classified within each gene ontology (GO) term were retrieved using the BioMart package for Bioconductor in R (Durinck et al., 2009; Gentleman et al., 2004). FPKM data corresponding to gene symbols within a GO term were retrieved from the normalized dataframe if the ANOVA P-value was < 0.05 for the comparison among the three sample groups and mean FPKM was greater than 1 in at least one of the three sample groups. Thus, downstream gene ontology analysis included only genes which differed significantly in expression between the HIO, fetal, and adult samples and were reproducibly expressed in at least one sample group. Normalized Z-scores for each gene within a GO term that met the inclusion criteria for were calculated as follows:

$$z = (x - \mu) / \sigma$$

Where *x* is an FPKM value, μ is the mean FPKM among all samples in all three groups for a given gene, and σ is the standard deviation among all samples in all three groups for a given gene. Heatmaps and associated dendrograms were plotted in R using the function “heatmap.2” in the package gplots (Warnes et al., 2014).

Principal Component Analysis

The complete FPKM matrix, containing frequency counts for all 23,615 known genes for all 33 RNAseq samples, was evaluated using principle component analysis (PCA) to visualize and quantify multi-dimensional variation between samples. Of the 23,615 known human genes, 1,281 (5.4%) were not detected in the RNAseq analysis of any of the 33 samples. Data scaling was applied to give equal weight to each gene as an equal component of the variation between samples. Variance (σ) can be expected to be highly variable among the 22,334 expressed genes contained in the dataset; thus scaling is advisable. Note that scaling is precluded by the presence of zero/missing data. To permit data scaling, it was necessary to remove all genes for which σ is equal to zero across all samples as it would be impossible to scale the variation in the remaining 22,334 genes to σ = 0. The advantage of data scaling is that specific genes with wide variation, perhaps varying in expression by many orders of magnitude, do not outweigh genes that may vary comparatively little but nonetheless may have biological significance. Likewise, in the absence of data scaling, widely variable genes increase the apparent dissimilarity between two samples, which may in fact share similar levels of expression in a large number of other genes. Thus, the range of variation in expression of each gene is normalized across samples such that each gene carries the same weight in the PCA. Data was not centered to avoid distortion of the axis regarding up- vs. down-regulation of transcription. Principle components were calculated using the function ’prcomp’ found in the R (version 3.1.2) statistical programming language (R Core Team, 2014) and plotted using the R package ’ggplot2’ (Wickham,

2009).

Hierarchical Clustering

Hierarchical cluster analysis based on the Canberra distance (Lance and Williams, 1966) between FPKM vectors was used to classify discrete RNAseq samples according to the degree of total transcriptional dissimilarity indicated by the normalized FPKM values. Bootstrap analysis was used to assess the uncertainty in the assigned hierarchical clustering relationships. 10,000 bootstraping iterations were generated by repeatedly randomly sampling the FPKM dataset. The bootstrap probability (BP) of a cluster is defined as the frequency of a given relationship among the bootstrap replicates. Multiscale bootstrap resampling was used to calculate an approximately unbiased (AU) *p*-value for a given relationship, with AU > 95 indicating a high degree of statistical significance. Analyses were conducted using R package 'pvclust' (Suzuki and Shimodaira, 2006).

The Canberra distance is a variation of the Spearman correlation that slightly penalizes the ranked comparisons with the greatest differences (Jurman et al., 2009). This method has been justified in genomics as a correction for intra-experimental variation, which in this experiment could be differences in the cell types present in HIO compared to fetal samples. HIOs contain only epithelium and mesenchyme and lack additional components such as neuronal, vascular, and immune cells that are present in the human fetal stomach and small intestine. The Canberra distance method may therefore exaggerate apparent differences thus resulting in a dendrogram (Fig. 1B) in which fetal small intestine and fetal stomach appear more related than HIOs and fetal small intestine.

Spearman Correlation

Spearman correlation was applied as an additional assessment of the cumulative degree of correlation among RNAseq datasets. We computed Spearman rank correlation coefficients (ρ) in a pairwise manner among all RNAseq samples using the complete normalized FPKM data. The Spearman coefficients were plotted as a heatmap using the function 'heatmap.2' in the R package 'gplots' (Warnes, 2014).

qRT-PCR

RNA was extracted from H9 embryonic stem cells, HIOs, tHIOs, and adult small intestine using the Trizol (Life Technologies) extraction protocol from the manufacturer. cDNA was generated using SuperScript®Vilo™ reverse transcriptase (Life Technologies) and qRT-PCR reactions were carried out using QuantiTect Sybr® Green (Qiagen). All reactions were run with 40 cycles of 95°C for 15 seconds, 55°C for 30 seconds, and 72°C for 45 seconds, followed by a melt curve of 95°C for 15 seconds, 60°C for 1 minute and then increasing temperature up to 95°C at 0.5 degree increments. Primer Sequences used are shown in Table S8.

Microscopy

Frozen or paraffin sections of HIOs, tHIOs, human small intestine, and mouse intestine were stained according to standard immunofluorescence and immunohistochemistry protocols. Generally, samples were blocked and permeabilized with PBS containing 5% donkey serum and 0.5% Triton-X 100. Primary antibodies were applied overnight at 4°C in 5% donkey serum and 0.05% Tween20/PBS. Lysozyme staining required antigen retrieval on both frozen and paraffin sections. For OLFM4 staining, tissues were incubated with primary antibody for 1 hr at room temperature. See Table S9 for a list of antibodies used. Alexa Fluor® conjugated secondary antibodies (Life Technologies) were then applied for 1 hr in 5% donkey serum/0.05% Tween20/PBS. Nuclei were stained with DAPI and mounted with ProLong® Gold antifade mountant (Life Technologies). Ki67 staining was done using a TSA kit (Life Technologies). All images were taken on an Olympus IX71 epifluorescent microscope, Nikon A1 confocal microscope, or a Hitachi H7600 transmission electron microscope. All post acquisition image processing (brightness and contrast) was applied uniformly to all comparable images.

LGR5 *in situ* hybridization

HIO, tHIO, and adult paraffin sections were sent to Advanced Cell Diagnostics for their RNAScope® *in situ* hybridization services. Samples were processed according to their publicly available standard protocol using their RNAScope® 2.0 High Definition Red Kit and returned for subsequent imaging. Images were taken on an Olympus BX-51 light microscope using a 100X objective.

Supplemental References

Ashburner, M., Ball, C.A., Blake, J.A., Botstein, D., Butler, H., Cherry, J.M., Davis, A.P., Dolinski, K., Dwight, S.S., Eppig, J.T., et al. (2000). Gene ontology: tool for the unification of biology. The Gene Ontology Consortium. Nat. Genet. *25*, 25–29.

Bell, S.M., Schreiner, C.M., Wert, S.E., Mucenski, M.L., Scott, W.J., and Whitsett, J.A. (2008). R-spondin 2 is required for normal laryngeal-tracheal, lung and limb morphogenesis. Development *135*, 1049–1058.

Chen, C., Khaleel, S.S., Huang, H., and Wu, C.H. (2014). Software for pre-processing Illumina next-generation sequencing short read sequences. Source Code for Biology and Medicine *9*, 8.

Durinck, S., Spellman, P.T., Birney, E., and Huber, W. (2009). Mapping identifiers for the integration of genomic datasets with the R/Bioconductor package biomaRt. Nat Protoc *4*, 1184–1191.

Gentleman, R.C., Carey, V.J., Bates, D.M., Bolstad, B., Dettling, M., Dudoit, S., Ellis, B., Gautier, L., Ge, Y., Gentry, J., et al. (2004). Bioconductor: open software development for computational biology and bioinformatics. Genome Biol *5*, R80.

Jurman, G., Riccadonna, S., Visintainer, R., and Furlanello, C. (2009). Canberra distance on ranked lists. Proceedings, Advances in Ranking-NIPS 09 Workshop 22–27.

Langmead, B., Trapnell, C., Pop, M., and Salzberg, S.L. (2009). Ultrafast and memory-efficient alignment of short DNA sequences to the human genome. Genome Biol. 10: R25.

Suzuki, R., and Shimodaira, H. (2006). Pvclust: an R package for assessing the uncertainty in hierarchical clustering. Bioinformatics *22*, 1540–1542.

Trapnell, C., Pachter, L., and Salzberg, S.L. (2009). TopHat: discovering splice junctions with RNA-Seq. Bioinformatics *25*, 1105–1111.

Trapnell, C., Hendrickson, D.G., Sauvageau, M., Goff, L., Rinn, J.L., and Pachter, L. (2013). Differential analysis of gene regulation at transcript resolution with RNA-seq. Nature Biotechnology *31*, 46–53.

Warnes, G.R., Ben Bolker, Bonebakker, L., Gentleman, R., Liaw, W.H.A., Lumley, T., Maechler, M., Magnusson, A., Moeller, S., Schwartz, M., et al. (2014). gplots: Various R programming tools for plotting data.

Wickham, H. (2009). ggplot2 (New York, NY: Springer New York).